arXiv:1401.7200v1 [hep-th] 28 Jan 2014

RIKEN-MP-83

Seiberg Duality, 5d SCFTs and Nekrasov Partition Functions

Masato Taki

Mathematical Physics Lab., RIKEN Nishina Center,
Saitama 351-0198, Japan

taki@riken.jp

Abstract

It is known that a 4d $\mathcal{N} = 1$ SCFT lives on D3-branes probing a local del Pezzo Calabi-Yau singularity. The Seiberg (or toric) duality of this SCFT arises from the Picard-Lefshetz transformation of the affine E_N 7-brane background that is associated with the Calabi-Yau threefold. In this paper we study the duality of the affine E_N background itself and a 5-brane probing it. We then find that many different Type IIB 5-brane webs describe the same SCFT in 5d. We check this duality by comparing the Nekrasov partition functions of these 5-brane web configurations.

1 Introduction

Developments in string theory have led to the existence of a great number of non-trivial interacting conformal field theories, which are not apparent from the framework of perturbative quantum field theory. Superconformal field theories (SCFTs) in five dimensions (5d) are typical examples. In general, 5d gauge theory is non-renormalizable and trivial, and such a theory cannot be a fundamental microscopic theory. However, by employing superstring theory, Seiberg [1] provided evidences of the existence of many non-Gaussian fixed point in 5d. The relevant deformation of such CFT flows to certain 5d $\mathcal{N} = 1$ gauge theory, and actually this gauge theory is non-perturbatively well-defined in spite of seeming non-renormalizability.

These 5d SCFTs, which are ultraviolet (UV) fixed point theories of 5d $\mathcal{N} = 1$ gauge theories, were studied from various viewpoints: Type I'/heterotic duality [1, 2], M-theory on a Calabi-Yau singularity [3, 4], Type IIB 5-brane web configuration [5, 6, 7] and Type IIB 7-brane background [8, 9, 10, 11]. In this paper, we employ the Calabi-Yau compactification, 5-brane web and 7-brane realization in order to study 5d SCFTs, and we then find that the branch cut move (the Picard-Lefshetz transformation) [12, 13, 14, 15, 16] of 7-brane configurations leads to non-trivial duality between web configurations of Calabi-Yau manifolds, and therefore the corresponding 5d SCFTs. This duality in 5d is deeply related to the Seiberg duality between 4d quiver gauge theories which are realized as worldvolume theories of D3-branes on Calabi-Yau singularities.

Let us consider two equivalent Calabi-Yau singularities that are related through 7-brane move. It was observed that two 4d gauge theories on D3-branes probing them are Seiberg-dual to each other [17, 18, 19, 20, 21, 22, 23, 24, 25]. In this sense, our duality between these Calabi-Yau manifolds is a parent of this 4d Seiberg duality. As we will explain, a generic dual pair of Calabi-Yau manifolds are not completely equivalent because these compactifications lead to decoupled extra states [26, 27, 28, 29, 30]. In 5d duality, we have to remove this extra contribution to formulate the duality, but the 4d Seiberg duality is very simple since a D3-brane world-volume theory does not feel these extra degrees of freedom.

In this paper we study the 5d field theories arising from M-theory compactified on the local del Pezzo surfaces $dP_{1,2,\cdots,6}$. In general, a local del Pezzo surface is not toric, and therefore we do not have efficient way to compute the corresponding partition function.

If a Calabi-Yau is toric, we can utilize the topological vertex formalism [31, 32, 33, 34, 35, 36, 37, 38, 39, 40] to calculate exactly its partition function. For a local del Pezzo surface, we find local pseudo del Pezzo surfaces $PdP_k^{p=I,II,\cdots}$ that are toric and dual to the local del Pezzo surface dP_k. We then conjecture that the del Pezzo partition function is given by the toric partition functions of the pseudo del Pezzo surfaces through the simple relation

$$Z_{dP_k} = \frac{Z_{PdP_k^p}}{Z_{\text{extra}}^{PdP_k^p}}, \quad p = I,\, II,\, \cdots, \tag{1.1}$$

where p labels the corresponding pseudo del Pezzo surfaces. The point is that the discrepancy between dP_k and PdP_k^p is only an overall factor $Z_{\text{extra}}^{PdP_k^p}$ in all cases. This extra factor arises from the above-mentioned extra states in the 5d spectrum, which do not transform correctly under the 5d Lorentz group. In this paper, we show that this nontrivial relation actually holds for all possible cases $dP_{1,2,\cdots,6}$.

This paper is organized as follows. We give a brief review on 5d field theories associated with 5-brane web configurations in section 2. In section 3, we study the relation between web configurations by employing 7-brane picture of local Calabi-Yau compactification. We then conjecture new relation between the Nekrasov partition functions of the Calabi-Yau manifolds associated with a del Pezzo surface. In section 4 we check this conjecture based on instanton expansion. We conclude in section 5. In appendix A and B, we set some conventions, deriving useful formulas.

2 Five-dimensional theories and 5-brane webs

5d $\mathcal{N} = 1$ $SU(2)$ gauge theories and their UV fixed point SCFTs are our main focus in this paper. We have many stingy realizations of such SCFTs and corresponding gauge theories. A well-known method to derive these fields theories from a string setup is using the (p, q) 5-brane web configurations in Type IIB superstring theory [5, 6, 8].

By considering $SL(2, \mathbb{Z})$ duality acting on a D5-brane, we can find there exists a (p, q) 5-brane with generic Ramond-Ramond and NS-NS charges. Let us consider the planar web configurations of these 5-branes. We assume that $x^{0,1,\cdots,4}$-dimensions are shared by all 5-branes and these 5-branes form a planar graph in the x^5-x^6 plane. A generic web is constructed by gluing trivalent vertex of three (p_i, q_i) 5-branes. Because of the charge

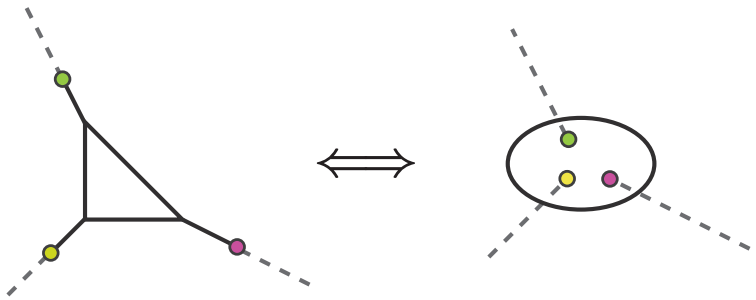

Figure 1: *The left hand side is the 5-brane web dual to the local $\mathbb{CP}^2$ geometry. We regularize an external leg by terminating it on a 7-brane. A colored circle is a 7-brane, and a dashed lines is branch cut arising from it. Moving these three 7-branes inside the 5-brane loop yields the right hand side through the Hanany-Witten effect.*

conservation, we have to impose

$$\sum_{i=1}^{3} p_i = 0 = \sum_{i=1}^{3} q_i. \tag{2.1}$$

To maintain a quarter of the original 32 supercharges, we have to impose the condition that the slope of a 5-brane in a planar diagram is given by its charge vector (p_i, q_i)[1]. We then find 5d $\mathcal{N} = 1$ field theories on their world-volumes.

M-theory compactified on a toric Calabi-Yau manifold also gives 5d $\mathcal{N} = 1$ theory. The toric Calabi-Yau three-folds are specified by the web diagrams up to $SL(2, \mathbb{Z})$ symmetry of their toric datas. An important fact is that a 5-brane web and the toric compactification specified by the same web diagram lead to the same stringy system because of string dualities. We can thus easily recast a 5-brane web system into the corresponding toric Calabi-Yau compactification. We therefore consider a web system without distinction between 5-brane configuration and toric Calabi-Yau geometry.

Let us consider an extension of these 5-brane systems. In Type IIB superstring theory, there exist 7-branes with generic (p, q) charges which originate from the $SL(2, \mathbb{Z})$ transformation of a D7-brane. We can terminate a 5-brane in a web on a 7-brane stretching to $x^{0,1,\cdots,4,7,8,9}$ directions [8]. This modification does not break supersymmetry, and moreover we can replace all external 5-brane legs with finite legs ending on 7-branes without

[1] In this convention, we consider the simple choice of the Type IIB coupling $\tau_{\rm IIB} = i$. The web diagrams take warped shapes in generic coupling, but this is irrelevant to our analysis.

changing the resulting 5d field theory[2]. This means that the 5d theory is independent of the lengths of these finite legs. ***Figure 1*** illustrates the 5-brane web of the local $\mathbb{CP}^2$ Calabi-Yau[3] modified by three 7-branes. The dashed lines are branch cuts created by 7-branes. Since 7-branes can move along the corresponding 5-brane legs, we can move all the 7-branes into the center of the web. When a 7-brane passes the 5-brane loop, the anti-Hanani-Witten mechanism occurs and the external leg attached to this 7-brane disappears. The resulting configuration is illustrated in the right hand side of ***Figure 1***. This system is a 5-brane loop proving a 7-brane background configuration. This representation as a 7-brane background configuration is not unique because a 7-brane changes its (p, q)-charges when it passes a branch cut of an another 7-brane. We can therefore find a different 7-brane configuration by changing the ordering of these 7-branes. This property of branch cut move plays a key role in our analysis. Some basic facts including the rule of branch cut move are reviewed in Appendix.A.

3 Toric phases of local (pseudo) del Pezzo surface

In this paper, we study the 5-brane web configurations with single loop. Since Type IIB superstring theory enjoys $SL(2,\mathbb{Z})$ duality, we consider only the $SL(2,\mathbb{Z})$-inequivalent configurations. The reflection is also irrelevant to our analysis, we consider the general linear group duality transformation

$$GL(2,\mathbb{Z}) = \left\{ \begin{pmatrix} a & b \\ c & d \end{pmatrix} \middle| ad - bc = \pm 1,\ a, b, c, d \in \mathbb{Z} \right\}. \tag{3.1}$$

We can classify the $GL(2,\mathbb{Z})$-inequivalent webs by considering the dual grid diagrams as ***Figure 2***. There are sixteen inequivalent convex lattice polygons with single internal point, and this means that there are sixteen inequivalent physical systems in Type IIB. These web configurations are illustrated in ***Figure 2***. The web with three external legs corresponds to the local $\mathbb{CP}^2$ geometry and does not associated with 5d gauge theory. We therefore consider the remaining webs.

[2]As we will see in this paper, the cases involving adjoining parallel legs are exceptions.

[3]Since a 5-brane web is dual to the toric Calabi-Yau for the same web diagram we call the 5-brane web by the name of the Calabi-Yau.

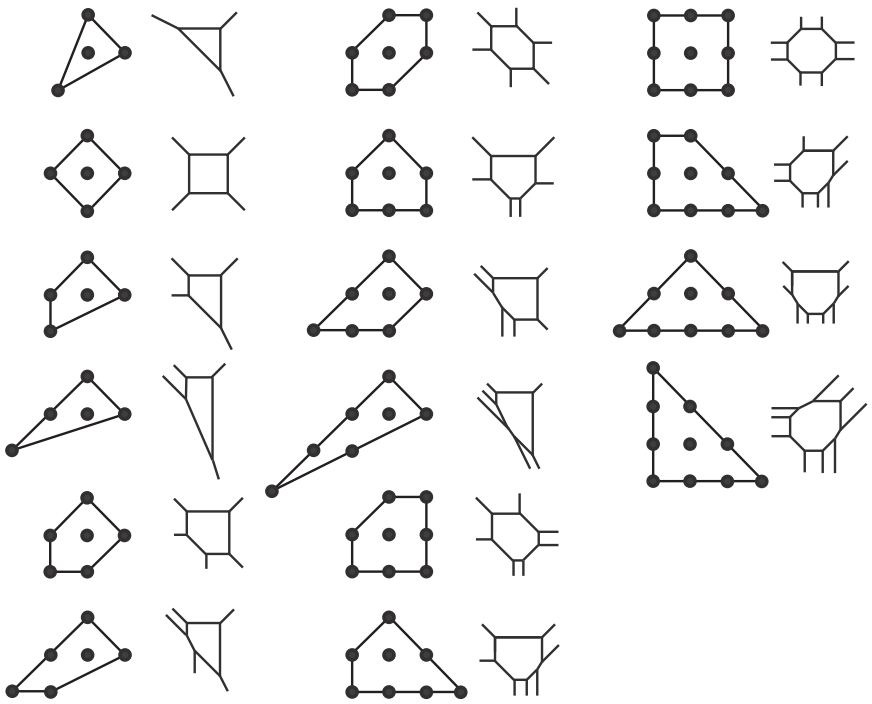

Figure 2: *All the $GL(2,\mathbb{Z})$-inequivalent convex lattice polygons with single internal point and their dual web diagrams.*

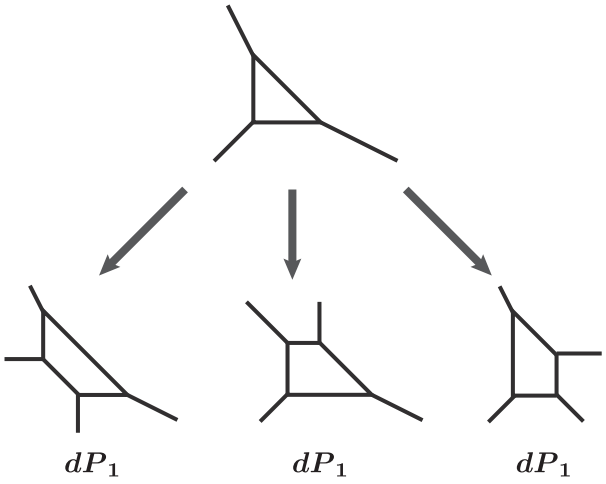

Figure 3: *Blowup in a toric web diagram. The local Calabi-Yau for the first del Pezzo $\mathcal{B}_1$ is the one point blowup of the local $\mathbb{P}^2$. The resulting three toric diagrams are equivalent up to the $SL(2,\mathbb{Z})$ symmetry transformation.*

In the studies on 4d quiver gauge theories [17, 18, 19, 20, 21, 22, 23, 24, 25], it was pointed out that some of these toric Calabi-Yau manifolds lead to Seiberg-dual pair of 4d theories. Recently, all the 4d $\mathcal{N}=1$ quiver gauge theories associated with these toric manifolds were determined in [41]. In this paper, we re-examine the relation between these toric manifolds from the recent perspectives of 5d SCFTs and related string setups, and then find new duality between Calabi-Yau compactifications of M-theory.

3.1 First del Pezzo surfaces dP_1 and $\widetilde{dP_1}$

The first del Pezzo surfaces correspond to the 5-brane webs in ***Figure 2*** with four external legs. These configurations describe 5d theories whose flavor symmetry is rank-one. There are three webs, however, there are only two known 5d SCFT with rank-one flavor symmetry. In the following we explain the origin of this mismatch by showing two of these three webs are actually dual to each other.

dP_1: local $\mathcal{B}_1$ (or $\mathbb{F}_1$) surface

The first del Pezzo surface $\mathcal{B}_1$ is the one point blowup of $\mathbb{CP}^1$. Using the $SL(3,\mathbb{C})$ symmetry on $\mathbb{CP}^1$, we can move three generic points to the three corners in the toric diagram

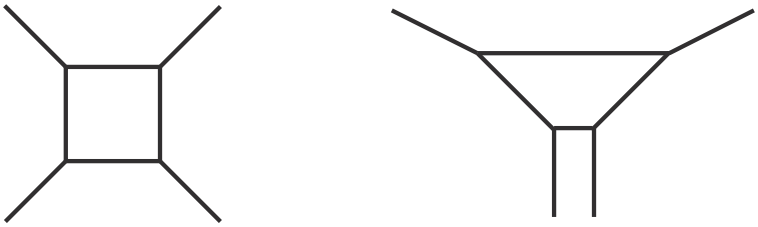

$\widetilde{dP_1}$ $P\widetilde{dP_1}$

Figure 4: *The two toric phases of the local geometry of the another first del Pezzo* $\tilde{\mathcal{B}}_1$.

without loss of generality. The local $\mathcal{B}_1$ Calabi-Yau threefold is given by the blowup of the toric web diagram of the local $\mathbb{CP}^1$ as ***Figure 3***. The three choices of blowup point lead to three local del Pezzo dP_1. Since a toric diagram specifies the corresponding Calabi-Yau threefold up to the action of $SL(2,\mathbb{Z})$ symmetry transformation. The three webs in ***Figure 3*** are actually the same geometry, and so there is only the unique toric phase of the local first del Pezzo surface. This toric geometry is also known as the local Hirzebruch surface $\mathbb{F}_1$. The compactification of M-theory on this Calabi-Yau manifold yields the 5d $\hat{E}_1$ SCFT [1, 3] whose flavor symmetry is $U(1)$.

$\widetilde{dP_1}$: local $\tilde{\mathcal{B}}_1$ (or $\mathbb{F}_0$) surface

There is the another class of the first del Pezzo surface $\tilde{\mathcal{B}}_1$ that coincides with the Hirzebruch surface $\mathbb{F}_0 = \mathbb{CP}^1 \times \mathbb{CP}^1$. The symbol $\widetilde{dP}_1$ in this paper denotes the local $\mathbb{F}_0$ geometry whose web diagram is illustrated in the left side of ***Figure 4***. The recent work [26, 29] showed that other toric geometry $P\widetilde{dP}_1$ that is the local geometry of $\mathbb{F}_2$ leads to the same compactified string theory as that of $\widetilde{dP}_1$ after removing certain extra contribution. This conjecture is stated as the following equivalence between their BPS Nekrasov partition functions

$$Z_{\widetilde{dP}_1}(Q_F, u; t, q) = \frac{Z_{P\widetilde{dP}_1}(Q_F, u; t, q)}{Z_{\text{extra}}^{P\widetilde{dP}_1}(u; t, q)}. \tag{3.2}$$

Z_{extra} is the partition function of the extra contribution given in [29, 26]. $Q_F = e^{2ia}$ is the fugacity associated with the Cartan of the $SU(2)$ gauge group, that is the Coulomb branch parameter, and t and q are the exponentiated Ω-background parameters. The charge associated with the instanton current $J = *\text{tr}F \wedge F$ is counted by the instanton

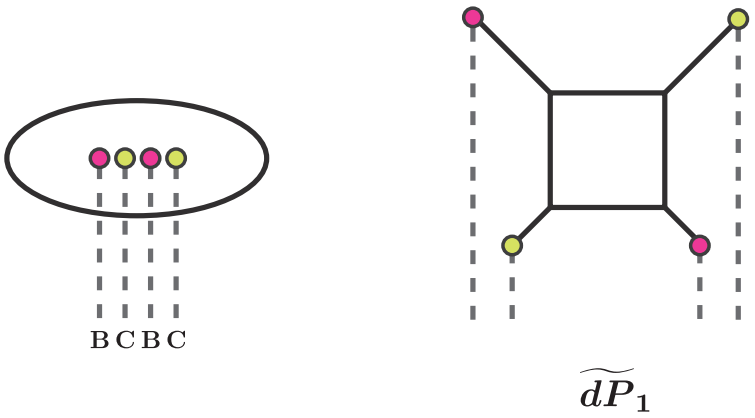

Figure 5: *The left hand side is the 5-brane loop probe of* $\hat{\mathbf{E}}_\mathbf{1}$ *7-brane configuration. Since all the 7-branes are not collapsible, only a sub-algebra* E_1 *is realized on the 5-brane. The right hand side is the corresponding web diagram which is obtained by moving a 7-brane the outside of the loop along the associated geodesic.*

factor u. The Nekrasov partition function for a toric Calabi-Yau threefold is computed by using the refined topological vertex formalism [37], and the algorithm to compute the corresponding extra contribution Z_{extra} for a given toric Calabi-Yau is given in [27, 28, 29]. We will review the check of the conjecture (3.2) in the next section.

This equivalence means that the 5d field theories arise from the two 5-brane web configurations, namely $\widetilde{dP}_1$ and $P\widetilde{dP}_1$, are the same quantum field theory up to essentially decoupled[4] extra contributions. We can actually derive the following equivalence between the superconformal indexes [42, 43] by using the conjectural relation (3.2)

$$I_{\widetilde{dP}_1} = \frac{I_{P\widetilde{dP}_1}}{I_{\text{extra}}}. \tag{3.3}$$

The web configurations therefore lead to the same 5d UV fixed point superconformal field theory E_1.

In the following, we will give a physical explanation of this non-trivial equivalence between these different Calabi-Yau compactifications and the corresponding 5d effective field theories. The key is the fact that a toric Calabi-Yau compactification of M-theory is dual the IIB 5-brane web configuration, and we can introduce the 7-branes on the edges

[4]Since the factorization (3.2) is satisfied by the Nekrasov partition function and superconformal index, the extra contribution is decoupled from the main 5d theory as far as the BPS sector is concerned.

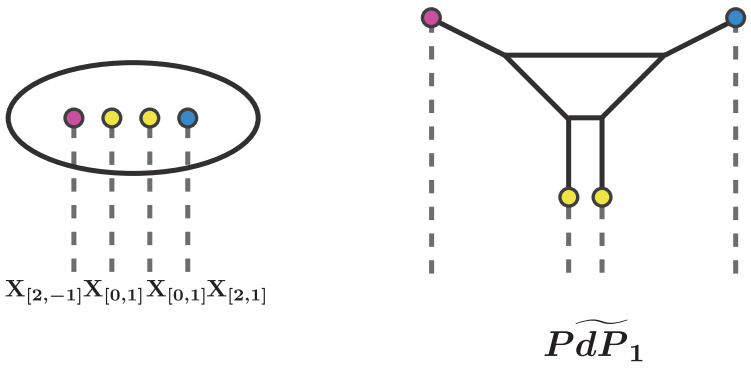

Figure 6: *The left hand side is the 5-brane loop probe of a reordered* $\hat{\mathbf{E}}_\mathbf{1}$ *7-brane configuration. The right hand side is the corresponding web diagram which is obtained by moving a 7-brane the outside of the loop. This is the web of* $P\widetilde{dP}_1$ *modified by four 7-branes.*

of the external 5-branes to make infinitely long external line finite length [8]. In the case of the local zeroth Hirzebruch $\widetilde{dP}_1$, the regularized 5-brane configuration is illustrated in the right side of ***Figure 5***. We introduce two types of 7-branes **B** and **C** to replacing the two types of the infinitely-long 5-branes into two types of finite 5-branes. A 7-brane creates a branch cut, and it is illustrated by the short dashed line in ***Figure 5***. In this figure we ignore a non-trivial metric created by the 7-brane background because only the asymptotic shape of web is important in our analysis.

The 5d field theory is independent of the length of the external legs. We can therefore move these 7-branes inside of the 5-brane loop. By using Hanany-Witten effect in an inverted way, we can see that the 5-brane prongs disappear when the 7-branes cross the 5-brane loop. The resulting configuration is illustrated in the left side of ***Figure 6***. This is the 5-brane loop probe of the 7-brane background **BCBC**. This 7-brane configuration is named as $\hat{\mathbf{E}}_1$

$$\hat{\mathbf{E}}_1 \equiv \mathbf{BCBC}. \tag{3.4}$$

In this paper, each branch cut extends downward from the base 7-brane except as otherwise specially provided. By reordering the 7-branes in this configuration, we can explain why the two local Hirzebruch surfaces give the same BPS spectrum and 5d field theory. Since a 7-brane creates the branch cut, reordering of 7-branes also transforms the

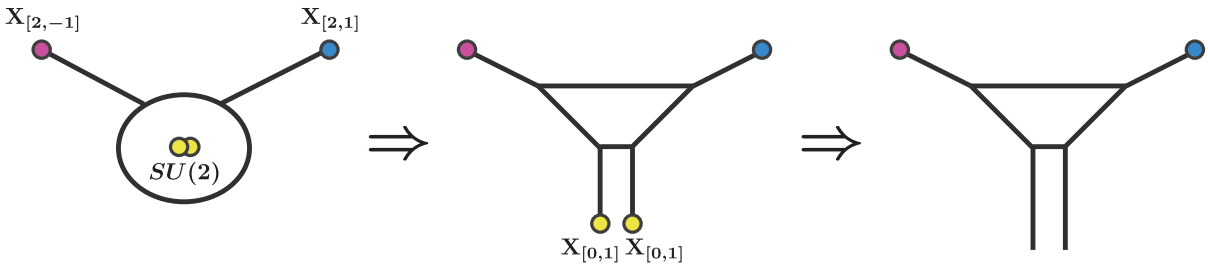

Figure 7: *If two* $\mathbf{X}_{[2,-1]}$ *branes move away to infinity, two adjoining parallel legs appear as illustrated in the right hand side. There exist extra states propagating along this infinitely-long additional dimension, and this resulting system therefore contains surplus spectrum.*

(p,q)-charges of them. The basic properties and rules are collected in Appendix.A. Let us move the 7-branes by using these rules. Starting with $\hat{\mathbf{E}}_1$ configuration, we find

$$\hat{\mathbf{E}}_1 \equiv \mathbf{BCBC} = \mathbf{BCCX}_{[3,1]} \overset{T^{-1}}{\simeq} \mathbf{X}_{[2,-1]}\mathbf{X}_{[0,1]}\mathbf{X}_{[0,1]}\mathbf{X}_{[2,1]}. \tag{3.5}$$

In the last equality we use the $SL(2,\mathbb{Z})$ dual transformtion

$$T = \begin{pmatrix} 1 & 0 \\ 1 & 1 \end{pmatrix}. \tag{3.6}$$

This new configuration is shown in the left hand side of ***Figure 6***. We can move the 7-branes outside of the loop, and we get the web diagram in the right hand side of ***Figure 6***. This is precisely the (toric) web diagram for the local second Hirzebruch $P\widetilde{dP}_1$ up to the 7-brane regularization.

This geometry $P\widetilde{dP}_1$ is not the genuine del Pezzo surface. We therefore call the base of this local geometry the pseudo first del Pezzo surface. This local pseudo del Pezzo surface $P\widetilde{dP}_1$ is a different geometry from the local del Pezzo $\widetilde{dP}_1$, however, these systems will be identical once the 7-branes are introduced in the dual 5-brane web picture.

We can remove $\mathbf{X}_{[2,-1]}$ and $\mathbf{X}_{[2,1]}$ branes safely, however we can not do $\mathbf{X}_{[0,1]}$ branes. This is because the attached prongs form the stack of two parallel 5-branes, and so new six-dimensional states appear once we move the 7-branes to infinity ***Figure 7***. In this sense the two toric phases $\widetilde{dP}_1$ and $P\widetilde{dP}_1$ are not completely identical, but the fact pointed out in [26, 27, 28, 29] is that the extra states are essentially decoupled from the

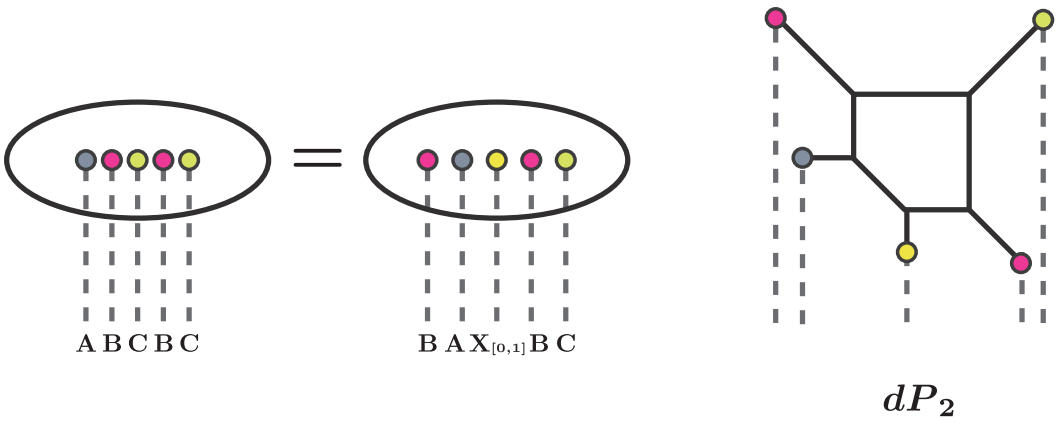

Figure 8: $\hat{\mathbf{E}}_2$ *configuration in the left hand side is equivalent to* $\mathbf{BAX}_{[0,1]}\mathbf{BC}$. *This configuration gives the web of* dP_2 *in the right hand side.*

5d theory and we can eliminate the extra contribution as (3.2). By generalizing this idea, we can find infinitely many dual toric phases which are related by the equivalence relation like (3.2). The phases discussed in the following provide simplest examples of such extension.

The trace of the monodormy matrix around $\mathbf{X}_{[0,1]}\mathbf{X}_{[0,1]}$ is

$$\mathrm{Tr}K_{[0,1]}K_{[0,1]} = 2, \tag{3.7}$$

and then $\mathbf{X}_{[0,1]}\mathbf{X}_{[0,1]}$ pair is collapsible as ***Figure 7***. In this picture this stack of 7-branes gives the enhanced $SU(2)$ symmetry, and therefore 5d field theory should lose this symmetry once these two branes are removed to obtain $P\widetilde{dP}_1$ toric geometry. Actually, the superconformal index $I_{P\widetilde{dP}_1}$ does not enjoy $SU(2)$ flavor symmetry, and we can recover the index $I_{\widetilde{dP}_1}$ with $SU(2)$ symmetry by removing the extra contribution.

3.2 Second del Pezzo surface dP_2

Toric del Pezzo phase dP_2

$\hat{\mathbf{E}}_2$ configuration is one-point blowup of $\hat{\mathbf{E}}_1$, and this blowup process is realized by adding an **A**-brane to the original 7-brane configuration. The resulting 7-brane configuration is

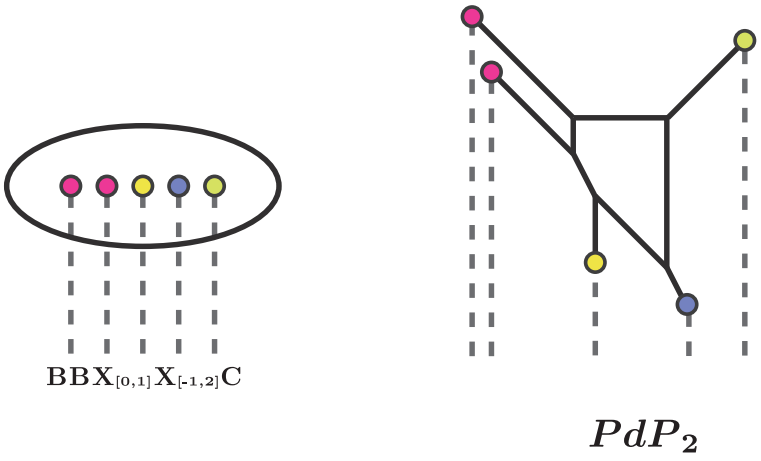

Figure 9: *$\hat{\mathbf{E}}_2$ configuration is also equivalent to $\mathbf{BBX}_{[0,1]}\mathbf{X}_{[-1,2]}\mathbf{C}$, and thus PdP_2 describes the same system as dP_2 once one add 7-branes to their webs.*

converted to $\mathbf{BAX}_{[0,1]}\mathbf{BC}$ by the action of the branch cut move for 7-branes

$$\begin{aligned}\hat{\mathbf{E}}_2 \equiv \mathbf{ABCBC} &= \mathbf{X}_{[0,-1]}\mathbf{ACBC} = \mathbf{BX}_{[0,-1]}\mathbf{CBC} = \mathbf{BCABC} \\ &= \mathbf{BAX}_{[0,1]}\mathbf{BC}.\end{aligned} \tag{3.8}$$

Pulling these five 7-branes out of the 5-brane loop creates new 5-brane prongs on the 7-branes through the Hanany-Witten effect. The resulting configuration is illustrated in ***Figure 8***. Moving along geodesics, all the 7-branes can run away to infinity without changing the 5d theory. The configuration then consists purely of 5-branes, and therefore it has dual toric Calabi-Yau geometry. This toric diagram, which has completely the same shape as the 5-brane web, is precisely that of the local second del Pezzo surface. Therefore, the $\hat{\mathbf{E}}_2$ background and the dP_2 Calabi-Yau lead to the same 5d theory.

Pseudo del Pezzo phase I PdP_2

We saw that the branch cut move of 7-branes converts $\hat{\mathbf{E}}_2$ background to dP_2 configuration. Applying successive move, we can find an another web representation of this configuration. Let us consider the following branch cut move

$$\hat{\mathbf{E}}_2 = \mathbf{BAX}_{[0,1]}\mathbf{BC} = \mathbf{BABX}_{[-1,2]}\mathbf{C} = \mathbf{BBX}_{[0,1]}\mathbf{X}_{[-1,2]}\mathbf{C}. \tag{3.9}$$

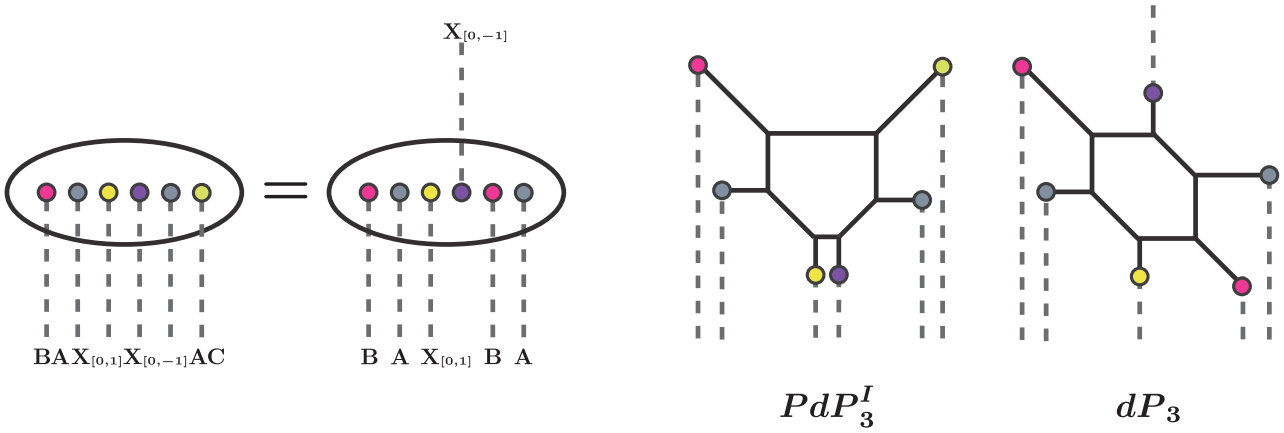

Figure 10: *dP_3 and PdP_3^I are related through branch cut move. Notice that the overall sign of the $[p,q]$ charge is irrelevant and so $\mathbf{X}_{[p,q]} = \mathbf{X}_{[-p,-q]}$. In this paper we do not replace $\mathbf{X}_{[-p,-q]}$ to $\mathbf{X}_{[p,q]}$ just for keeping track of the branch cut moves.*

This configuration $\mathbf{BBX}_{[0,1]}\mathbf{X}_{[-1,2]}\mathbf{C}$ leads to the web diagram for the pseudo del Pezzo phase I of the second del Pezzo surface as ***Figure 9***. Since the common 7-brane configuration $\hat{\mathbf{E}}_2$ produces the webs of dP_2 and PdP_2, these two webs yield precisely the equivalent 5d theory. Notice that the web configuration PdP_2 contains the stack of two parallel external legs terminated on **BB**. As we discussed in the previous subsection about $\widetilde{dP}_1$, we can not move the 7-branes on the parallel stack to infinity without changing the 5d theory. Therefore, the Nekrasov partition function of PdP_2, whose web configuration is obtained by removing all the 7-branes, can not perfectly coincide with that of dP_2 diagram. The discrepancy between them however takes very simple form as the cases studied in [26, 27, 28, 29], and so this mismatch is not essential. We then expect the following relation between the partition functions of these two phases

$$Z_{dP_2}(Q_F, u, Q_E; t, q) = \frac{Z_{PdP_2}(Q_F, u, Q_E; t, q)}{Z^{PdP_2}_{\text{extra}}(u, Q_E; t, q)}. \tag{3.10}$$

We will check this equivalence relation between the phases in the next section.

3.3 Third del Pezzo surface dP_3 and PdP_3

There are four phases of the third del Pezzo surface. The toric phase for the genuine third del Pezzo surface dP_3 is illustrated in the right hand side of ***Figure 11***. The web

diagram next to dP_3 in ***Figure 10*** is that for the first phase of the pseudo del Pezzo surface PdP_3^I. We will show they are identical once the 7-branes are introduced.

Toric dP_3 and pseudo del Pezzo phase I PdP_3^I

The third del Pezzo surface is the 5-brane loop probe of the $\hat{\mathbf{E}}_3$ 7-brane configuration. By moving branchs, cuts we obtain

$$\begin{aligned}\hat{\mathbf{E}}_3 &\equiv \mathbf{A}^2\mathbf{BCBC} \\ &= \mathbf{ABAX}_{[0,1]}\mathbf{BC} = \mathbf{BX}_{[0,1]}\mathbf{AX}_{[0,1]}\mathbf{BC} = \mathbf{BAX}_{[1,-1]}\mathbf{X}_{[0,1]}\mathbf{BC} = \mathbf{BAX}_{[0,1]}\mathbf{ABC} \\ &= \mathbf{BAX}_{[0,1]}\mathbf{X}_{[0,-1]}\mathbf{AC}, \end{aligned} \tag{3.11}$$

and this 7-brane configuration gives the web of the pseudo del Pezzo PdP_3^I. Moving the branch cut coming from the brane $\mathbf{X}_{[0,-1]}$ upward, we obtain

$$\mathbf{BAX}_{[0,1]}\mathbf{X}_{[0,-1]}\mathbf{AC} = \mathbf{BAX}_{[0,1]}\mathbf{X}_{[0,-1]}\mathbf{BA}\,. \tag{3.12}$$

This representation leads to the web of dP_3 as ***Figure 10***. The two toric phases dP_3 and PdP_3^I are therefore the equivalent brane configurations, and the partition functions become the same function once one factors the contribution from the stack of two parallel external branes out

$$Z_{dP_3} = \frac{Z_{PdP_3^I}}{Z_{\text{extra}}^{PdP_3^I}}, \qquad Z_{\text{extra}}^{PdP_3^I} = Z_{\text{parallel two 5-branes}}. \tag{3.13}$$

As we will see soon, this Z_{dP_3} partition function has different expressions based on other pseudo del Pezzo phases.

Pseudo del Pezzo phases II,III $PdP_3^{II,III}$

There are two remaining phases of the third del Pezzo. ***Figure 11*** and ***Figure 12*** are the pseudo third del Pezzo surfaces $PdP_3^{II,III}$. These phases are also equivalent to the local del Pezzo surface dP_3. We can show this fact by using the 7-brane picture again.

Let us start with the phase II of the pseudo third del Pezzo PdP_3^{II}. Branch cut move implies the relation

$$\begin{aligned}\mathbf{AX}_{[0,1]}\mathbf{X}_{[0,-1]}\mathbf{A} &= \mathbf{AX}_{[0,1]}\mathbf{BX}_{[0,-1]} = \mathbf{AX}_{[0,1]}\mathbf{X}_{[-1,0]}\mathbf{B} = \mathbf{AX}_{[-1,0]}\mathbf{X}_{[-1,1]}\mathbf{B} \\ &= \mathbf{AX}_{[-1,1]}\mathbf{X}_{[0,-1]}\mathbf{B} = \mathbf{X}_{[0,1]}\mathbf{AX}_{[0,-1]}\mathbf{B} = \mathbf{BX}_{[0,1]}\mathbf{X}_{[0,-1]}\mathbf{B}. \end{aligned} \tag{3.14}$$

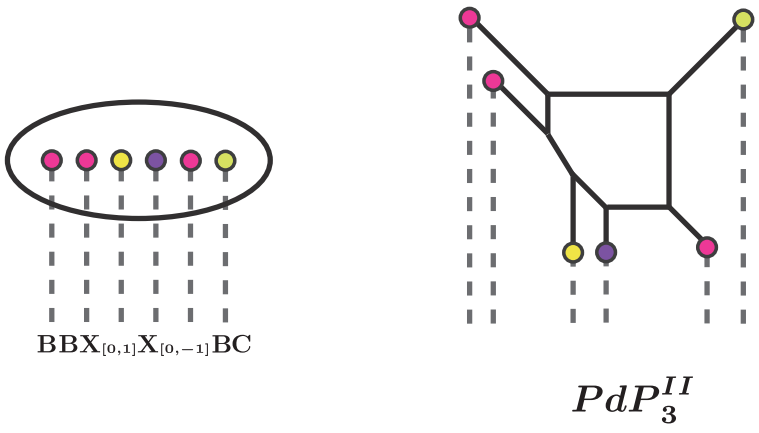

Figure 11: *dP_3 is equivalent to PdP_3^{II} that is associated with* $\mathbf{BAX}_{[0,1]}\mathbf{X}_{[0,-1]}\mathbf{BA}$.

We can therefore find the following expression for the $\hat{\mathbf{E}}_3$ configuration

$$\hat{\mathbf{E}}_3 = \mathbf{BAX}_{[0,1]}\mathbf{X}_{[0,-1]}\mathbf{AC} = \mathbf{BBX}_{[0,1]}\mathbf{X}_{[0,-1]}\mathbf{BC}. \tag{3.15}$$

Since the right hand side of this equation gives the PdP_3^{II} configuration as ***Figure 11***, this phase is equivalent to PdP_3^{I} and dP_3. Since there are two stacks of parallel external branes, the extra contribution to the PdP_3^{II} partition function takes the form

$$Z_{\text{extra}}^{PdP_3^{II}} = Z_{\text{parallel two 5-branes}} \times Z_{\text{parallel two 5-branes}}. \tag{3.16}$$

By factoring this extra contribution out, we obtain the dP_3 partition function from the PdP_3^{II} partition function

$$Z_{dP_3} = \frac{Z_{PdP_3^{II}}}{Z_{\text{extra}}^{PdP_3^{II}}}. \tag{3.17}$$

We can also show the equivalence between dP_3 and PdP_3^{III}. Branch cut move leads to the relation

$$\mathbf{X}_{[0,1]}\mathbf{X}_{[0,-1]}\mathbf{B} = \mathbf{X}_{[0,1]}\mathbf{B}\mathbf{X}_{[1,-2]} = \mathbf{B}\mathbf{X}_{[-1,2]}\mathbf{X}_{[1,-2]}, \tag{3.18}$$

and by applying it to (3.15), we obtain

$$\hat{\mathbf{E}}_3 = \mathbf{BBX}_{[0,1]}\mathbf{X}_{[0,-1]}\mathbf{BC} = \mathbf{BBBX}_{[-1,2]}\mathbf{X}_{[1,-2]}\mathbf{C}. \tag{3.19}$$

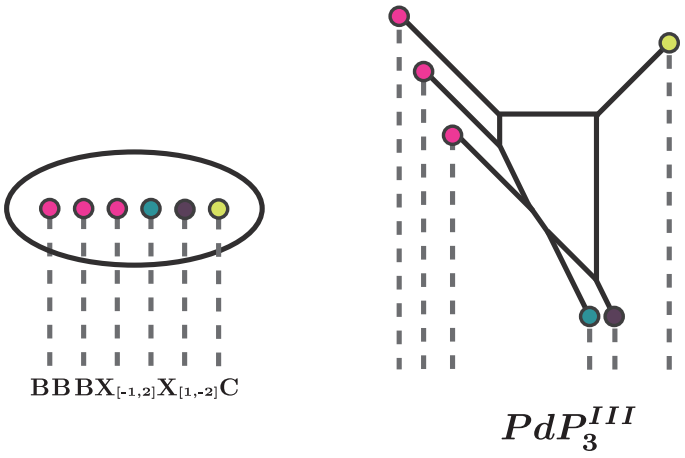

Figure 12: *dP_3 is equivalent to PdP_3^{III} that is associated with* $\mathbf{BBBX}_{[-1,2]}\mathbf{X}_{[1,-2]}\mathbf{C}$.

The right hand side of this equation gives the PdP_3^{III} configuration as ***Figure 12***. This phase is therefore equivalent to PdP_3^{II}, and therefore to dP_3. There are a stack of two parallel 5-branes and a stack of three parallel 5-branes, and PdP_3^{III} partition function consequently leads to the dP_3 partition function by factoring the following extra contribution $Z_{\rm extra}^{PdP_3^{III}}$ out

$$Z_{dP_3} = \frac{Z_{PdP_3^{III}}}{Z_{\rm extra}^{PdP_3^{III}}}, \quad Z_{\rm extra}^{PdP_3^{III}} = Z_{\text{parallel two 5-branes}} \times Z_{\text{parallel three 5-branes}}. \tag{3.20}$$

This equivalence is very non-trivial because the calculation of the PdP_3^{III} partition function is very hard. Computing instanton expansion of this partition function, our new conjecture is checked in the next section.

3.4 Fourth del Pezzo surface dP_4 and PdP_4

The local fourth del Pezzo surface dP_4 itself is non-toric and does not have any 5-brane web description. We can however construct toric analogue of it by blowing up the toric descriptions of the third pseudo del Pezzo surface dP_3, and there are two resulting toric phases $PdP_4^{I,II}$ for the local pseudo del Pezzo surface. By introducing the 7-brane regularization, we can show the equivalence between the pseudo del Pezzo surfaces PdP_4 and the genuine one dP_4.

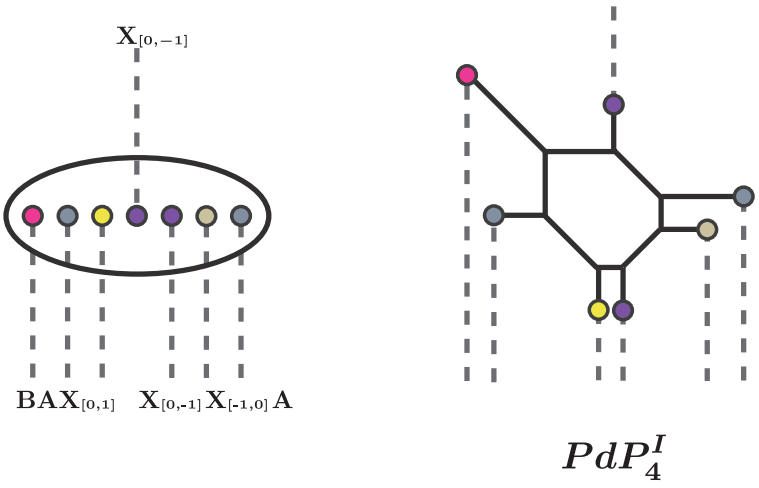

Figure 13: *$\hat{\mathbf{E}}_4$ configuration is related to $\mathbf{BAX}_{[0,1]}\mathbf{X}_{[0,-1]}\mathbf{X}_{[0,-1]}\mathbf{X}_{[-1,0]}\mathbf{C}$, and therefore dP_4 is equivalent to PdP_4^I.*

Pseudo del Pezzo phase I PdP_4^I

The local fourth del Pezzo surface is realized by the 5-brane probe of the $\hat{\mathbf{E}}_4$ configuration. By using (3.11), we get

$$\begin{aligned}\hat{\mathbf{E}}_4 &\equiv \mathbf{A}^3\mathbf{BCBC} = \mathbf{ABAX}_{[0,1]}\mathbf{X}_{[0,-1]}\mathbf{AC} = \mathbf{BX}_{[0,1]}\mathbf{AX}_{[0,1]}\mathbf{X}_{[0,-1]}\mathbf{AC} \\ &= \mathbf{BAX}_{[-1,1]}\mathbf{X}_{[0,1]}\mathbf{X}_{[0,-1]}\mathbf{AC} = \mathbf{BAX}_{[0,1]}\mathbf{X}_{[-1,0]}\mathbf{X}_{[0,-1]}\mathbf{AC},\end{aligned} \tag{3.21}$$

and we find the following expression by moving the branch cut coming from $\mathbf{X}_{[0,-1]}$ upward

$$\begin{aligned}\hat{\mathbf{E}}_4 &= \mathbf{BAX}_{[0,1]}\mathbf{X}_{[-1,0]}\mathbf{X}_{[0,-1]}\mathbf{BA} = \mathbf{BAX}_{[0,1]}\mathbf{X}_{[0,-1]}\mathbf{X}_{[-1,0]}\mathbf{BA} \\ &= \mathbf{BAX}_{[0,1]}\mathbf{X}_{[0,-1]}\mathbf{X}_{[0,-1]}\mathbf{X}_{[-1,0]}\mathbf{A} \quad .\end{aligned} \tag{3.22}$$

The last expression immediately gives the pseudo del Pezzo PdP_4^I as illustrated in ***Figure 13***. Therefore this pseudo del Pezzo is equivalent to the genuine del Pezzo dP_4 once one introduces the 7-brane regularization to all the external legs. This pseudo del Pezzo phase contains two stacks of two parallel 5-branes, and so we can obtain the dP_4 partition

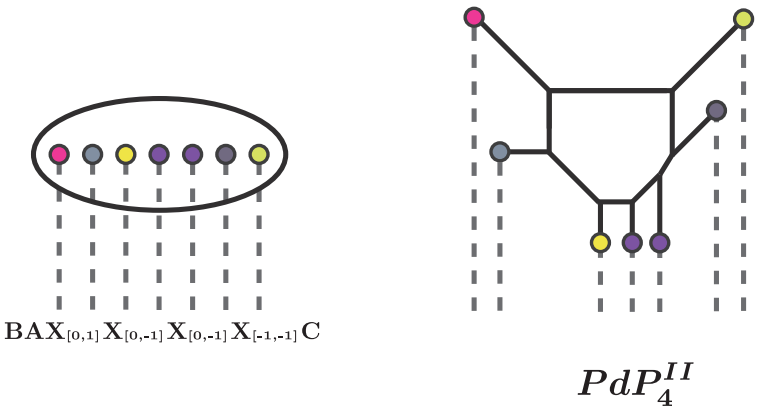

Figure 14: *dP_4 is equivalent to PdP_4^{II}. This 5-brane web is associated with the 7-brane configuration* $\mathbf{BAX}_{[0,1]}\mathbf{X}_{[0,-1]}\mathbf{X}_{[0,-1]}\mathbf{X}_{[-1,-1]}\mathbf{C}$.

function by removing the following extra factor from the PdP_4^I partition function

$$Z_{dP_4}(Q_F, u, Q_{Ef}; t, q) = \frac{Z_{PdP_4^I}(Q_F, u, Q_{Ef}; t, q)}{Z_{\text{extra}}^{PdP_4^I}(u, Q_{Ef}; t, q)}, \tag{3.23}$$

$$Z_{\text{extra}}^{PdP_4^I} = Z_{\text{parallel two 5-branes}} \times Z_{\text{parallel two 5-branes}}. \tag{3.24}$$

This conjecture was checked at the level of the superconformal index [27, 28], and the authors showed that the renormalized PdP_4^I partition function leads to the index with the enhanced E_4 symmetry which is expected from property of the del Pezzo surface dP_4.

Pseudo del Pezzo phase II PdP_4^{II}

For the fourth del Pezzo surface, we can employ the additional toric phase PdP_4^{II} illustrated in ***Figure 14***. This pseudo del Pezzo surface is also equivalent to the del Pezzo dP_4 as follows. By using the relation (3.21), we find

$$\begin{aligned}\hat{\mathbf{E}}_4 &= \mathbf{BAX}_{[0,1]}\mathbf{X}_{[-1,0]}\mathbf{X}_{[0,-1]}\mathbf{AC} = \mathbf{BAX}_{[0,1]}\mathbf{X}_{[0,-1]}\mathbf{X}_{[-1,-1]}\mathbf{AC} \\ &= \mathbf{BAX}_{[0,1]}\mathbf{X}_{[0,-1]}\mathbf{X}_{[0,-1]}\mathbf{X}_{[-1,-1]}\mathbf{C}. \end{aligned} \tag{3.25}$$

The last line is precisely the 7-brane configuration that leads to PdP_4^{II} as ***Figure 14***.

This pseudo del Pezzo surface contains a stack of two parallel 5-branes and a stack of three parallel 5-branes, and therefore the dP_4 partition function is the PdP_4^{II} partition

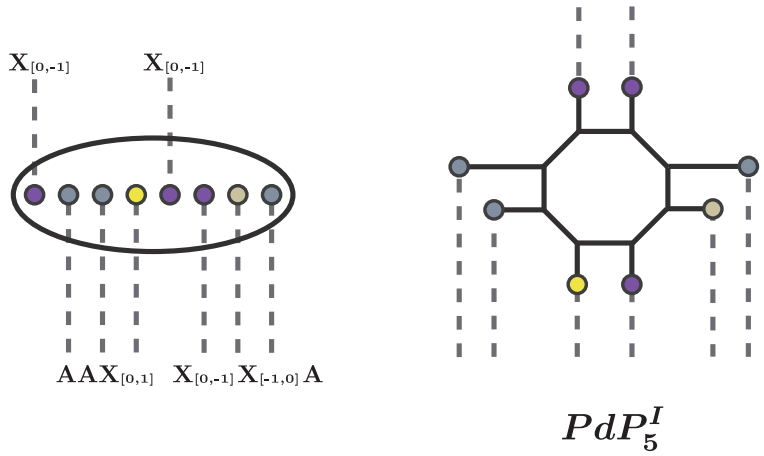

Figure 15: *Moving branch cuts of* $\hat{\mathbf{E}}_5$ *configuration, we obtain the configuration on the left side. The pseudo del Pezzo surface illustrated on the right side is thus equivalent to* dP_5.

function divided by the following extra factor

$$Z_{dP_4}(Q_F, u, Q_{Ef}; t, q) = \frac{Z_{PdP_4^{II}}(Q_F, u, Q_{Ef}; t, q)}{Z_{\text{extra}}^{PdP_4^{II}}(u, Q_{Ef}; t, q)}, \tag{3.26}$$

$$Z_{\text{extra}}^{PdP_4^{II}} = Z_{\text{parallel two 5-branes}} \times Z_{\text{parallel three 5-branes}}. \tag{3.27}$$

This new conjecture is checked in the next section.

3.5 PdP_5

The local fifth del Pezzo surface dP_4 is not toric, and therefore it does not have 5-brane web description. We can, however, construct pseudo del Pezzo surfaces as the previous cases, and there are three toric pseudo del Pezzo phases $PdP_5^{I,II,II}$. By introducing the 7-brane regularization, we can show that these pseudo del Pezzo surfaces lead to the same compactification of superstring theory as that on the non-toric del Pezzo dP_5.

Pseudo del Pezzo phase I PdP_5^I

Let us start with the pseudo del Pezzo surface PdP_5^I illustrated in ***Figure 15***. We can regularize the corresponding 5-brane web by introducing two types of 7-branes $\mathbf{A}$ =

$\mathbf{X}_{[-1,0]}$ and $\mathbf{X}_{[0,1]} = \mathbf{X}_{[0,-1]}$. We can show that this configuration is equivalent to the local fifth del Pezzo surface associated with $\hat{\mathbf{E}}_5$ configuration

$$\hat{\mathbf{E}}_5 \equiv \mathbf{A}^4\mathbf{BCBC} = \mathbf{ABAX}_{[0,1]}\mathbf{X}_{[-1,0]}\mathbf{X}_{[0,-1]}\mathbf{AC} = \mathbf{X}_{[0,-1]}\mathbf{AAX}_{[0,1]}\mathbf{X}_{[-1,0]}\mathbf{X}_{[0,-1]}\mathbf{AC}. \tag{3.28}$$

We use (3.21) to show the second equality. By moving the branch cut as (3.12), we obtain

$$\hat{\mathbf{E}}_5 = \mathbf{X}_{[0,-1]}\mathbf{AAX}_{[0,1]}\overbrace{\mathbf{X}_{[0,-1]}\mathbf{X}_{[0,-1]}\mathbf{X}_{[0,-1]}\mathbf{A}}, \tag{3.29}$$

and this expression leads to the pseudo del Pezzo surface as ***Figure 15***. This toric phase contains four stacks of four parallel 5-branes and the extra contribution from the non-full spin content is

$$Z_{dP_5}(Q_F, u, Q_{Ef}; t, q) = \frac{Z_{PdP_5^I}(Q_F, u, Q_{Ef}; t, q)}{Z_{\text{extra}}^{PdP_5^I}(u, Q_{Ef}; t, q)}, \tag{3.30}$$

$$\begin{aligned} Z_{\text{extra}}^{PdP_5^I} &= Z_{\text{parallel two 5-branes}} \times Z_{\text{parallel two 5-branes}} \\ &\quad \times Z_{\text{parallel two 5-branes}} \times Z_{\text{parallel two 5-branes}}. \end{aligned} \tag{3.31}$$

By removing this extra contribution, we can obtain the Nekrasov partition function of the local del Pezzo surface dP_5 from the pseudo del Pezzo partition function. This conjecture was checked in [27, 28] based on the explicit computation.

Pseudo del Pezzo phase II PdP_5^{II}

There are another toric phase of the del Pezzo dP_5. ***Figure 16*** is the second phase PdP_5^{II}. This phase is also equivalent to $\hat{\mathbf{E}}_5$ because branch cut move implies

$$\hat{\mathbf{E}}_5 = \mathbf{ABAX}_{[0,1]}\mathbf{X}_{[0,-1]}\mathbf{X}_{[0,-1]}\mathbf{X}_{[-1,-1]}\mathbf{C} = \mathbf{X}_{[0,-1]}\mathbf{AAX}_{[0,1]}\mathbf{X}_{[0,-1]}\mathbf{X}_{[0,-1]}\mathbf{X}_{[-1,-1]}\mathbf{C}. \tag{3.32}$$

To show the first equality we use the relation (3.25). The last 7-brane configuration leads to the second toric phase as illustrated in ***Figure 16***. This web configuration contains three stacks of infinitely-long external 5-branes once one remove the 7-brane regularization. The PdP_5^{II} partition function consequently coincides with the dP_5 partition

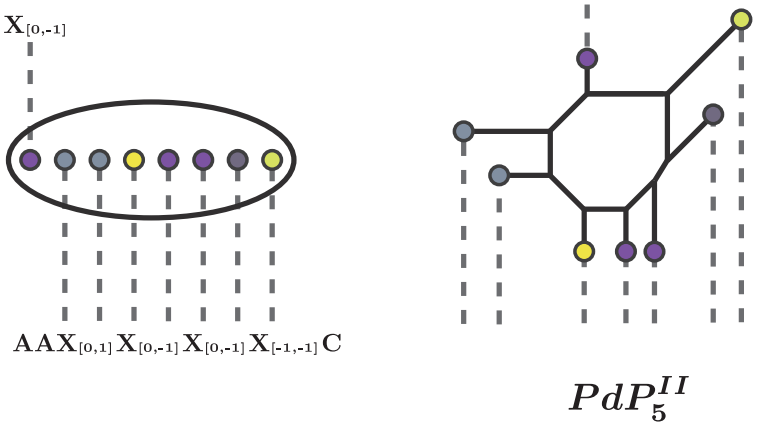

Figure 16: $\hat{\mathbf{E}}_5$ *configuration leads to the 7-brane configuration on the left side.* PdP_5^{II} *is therefore equivalent to* dP_5*.*

function after removing the extra contribution from the stacks as

$$Z_{dP_5}(Q_F, u, Q_{Ef}; t, q) = \frac{Z_{PdP_5^{II}}(Q_F, u, Q_{Ef}; t, q)}{Z^{PdP_5^{II}}_{\text{non-ful}}(u, Q_{Ef}; t, q)}, \tag{3.33}$$

$$Z^{PdP_5^{II}}_{\text{extra}} = Z_{\text{parallel three 5-branes}} \times Z_{\text{parallel two 5-branes}} \times Z_{\text{parallel two 5-branes}}. \tag{3.34}$$

This new conjecture is checked in the next section.

Pseudo del Pezzo phase III PdP_5^{III}

The third toric phase PdP_5^{III} is illustrated in ***Figure 17***. The following relation follows from branch cut move

$$\begin{aligned}\hat{\mathbf{E}}_5 &= \mathbf{ABAX}_{[0,1]}\mathbf{X}_{[0,-1]}\mathbf{X}_{[0,-1]}\mathbf{X}_{[-1,-1]}\mathbf{C} = \mathbf{BX}_{[0,1]}\mathbf{AX}_{[0,1]}\mathbf{X}_{[0,-1]}\mathbf{X}_{[0,-1]}\mathbf{X}_{[-1,-1]}\mathbf{C} \\ &= \mathbf{BBX}_{[0,1]}\mathbf{X}_{[0,1]}\mathbf{X}_{[0,-1]}\mathbf{X}_{[0,-1]}\mathbf{X}_{[-1,-1]}\mathbf{C},\end{aligned} \tag{3.35}$$

and the last line leads to the PdP_5^{III} brane web configuration as ***Figure 17***. Therefore this phase PdP_5^{III} is also equivalent to the genuine local del Pezzo surface in the presence of the 7-brane regularization.

By removing the 7-branes, we obtain the 5-brane web and can compute the corresponding partition function by using the refined topological vertex formalism. Once one takes away the 7-brane regularization, the stacks of the parallel external 5-branes develop extra contribution. The PdP_5^{III} partition function therefore coincides with the dP_5

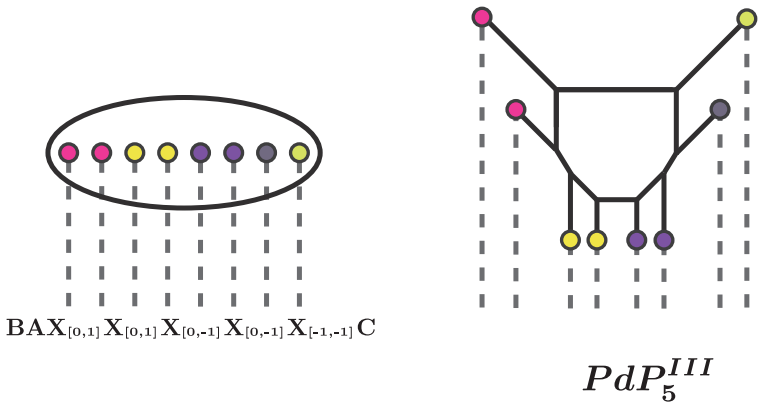

Figure 17: *$\hat{\mathbf{E}}_5$ configuration leads to the 7-brane configuration on the left side. PdP_5^{III} is therefore equivalent to dP_5.*

partition function after eliminating the extra contribution

$$Z_{dP_5}(Q_F, u, Q_{Ef}; t, q) = \frac{Z_{PdP_5^{III}}(Q_F, u, Q_{Ef}; t, q)}{Z_{\text{extra}}^{PdP_5^{II}}(u, Q_{Ef}; t, q)}, \tag{3.36}$$

$$Z_{\text{extra}}^{PdP_5^{III}} = Z_{\text{parallel four 5-branes}} \times Z_{\text{parallel two 5-branes}} \times Z_{\text{parallel two 5-branes}}. \tag{3.37}$$

This new conjecture is also checked in the next section.

3.6 PdP_6

The non-toric local fifth del Pezzo surface dP_5 does not have any 5-brane web description. There are however the toric pseudo del Pezzo phase PdP_6 illustrated in ***Figure 18***. We can relate the pseudo del Pezzo phase PdP_6 to the genuine del Pezzo dP_6 by moving branch cuts of the corresponding 7-brane background

$$\begin{aligned}\hat{\mathbf{E}}_6 \equiv \mathbf{A}^5\mathbf{BCBC} &= \mathbf{A}\mathbf{X}_{[0,-1]}\mathbf{A}\mathbf{A}\mathbf{X}_{[0,1]}\mathbf{X}_{[0,-1]}\mathbf{X}_{[0,-1]}\mathbf{X}_{[-1,-1]}\mathbf{C} \\ &= \mathbf{X}_{[-1,-1]}\mathbf{A}\mathbf{A}\mathbf{A}\mathbf{X}_{[0,1]}\mathbf{X}_{[0,-1]}\mathbf{X}_{[0,-1]}\mathbf{X}_{[-1,-1]}\mathbf{C}.\end{aligned} \tag{3.38}$$

The last line leads to the web of PdP_5 as ***Figure 18***.

Since the pseudo del Pezzo configuration contains three stacks of three parallel 5-branes, the PdP_6 partition function coincides with the dP_6 partition function after re-

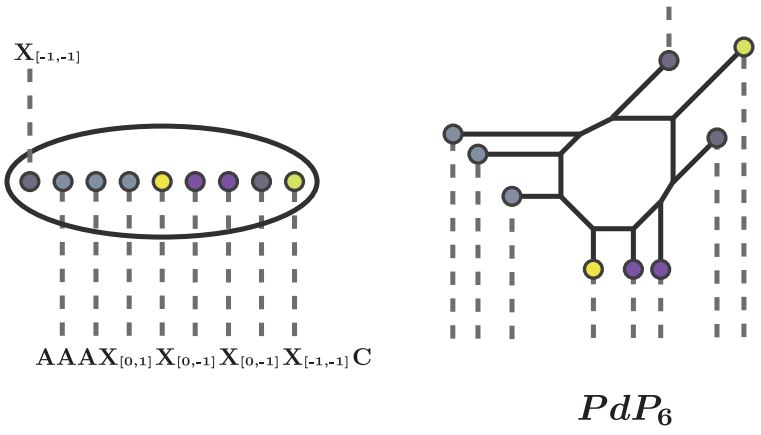

Figure 18: *Moving branch cuts of* $\hat{\mathbf{E}}_6$ *configuration, we obtain the configuration on the left side. The pseudo del Pezzo surface* PdP_6 *illustrated on the right side is thus equivalent to* dP_6*.*

moving the extra contribution arising from these stacks

$$Z_{dP_6}(Q_F, u, Q_{Ef}; t, q) = \frac{Z_{PdP_6}(Q_F, u, Q_{Ef}; t, q)}{Z_{\text{extra}}^{PdP_6}(u, Q_{Ef}; t, q)}, \tag{3.39}$$

$$Z_{\text{extra}}^{PdP_6} = Z_{\text{parallel three 5-branes}} \times Z_{\text{parallel three 5-branes}} \times Z_{\text{parallel three 5-branes}}. \tag{3.40}$$

This relation was conjectures in [27, 28]. The authors checked it by computing the corresponding superconformal index and confirming the enhancement of the E_6 flavor symmetry expected from the geometry of dP_6. This SCFT with E_6 flavor symmetry is precisely the 5d uplift of Gaiotto's T^3 theory [44, 45].

4 Nekrasov partition functions of del Pezzo suraces

In this section, we check explicitly our conjecture that the Nekrasov partition functions of the toric phases of a local del Pezzo surface lead to the same partition function that describes the local del Pezzo surface once the non-full spin content part is removed

$$Z_{dP_k} = \frac{Z_{PdP_k^p}}{Z_{\text{extra}}^{PdP_k^p}}, \quad p = I,\, II,\, III,\, \cdots, \tag{4.1}$$

where $Z_{\text{extra}}^{PdP_k^p}$ is the product of all the contributions from the stacks of parallel external legs. p labels the toric phases associated with the local del Pezzo surface dP_k. We can

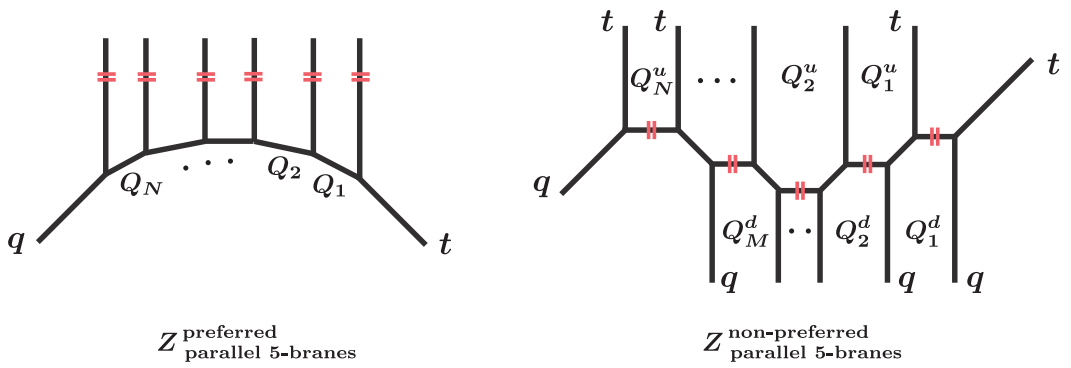

Figure 19: *The extra contributions of the non-full spin content.*

compute this extra part as follows. There are two types of stacks of parallel external 5-branes as illustrated in ***Figure 19***: one is the non-preferred external legs, and the other is the preferred external legs. These sub-diagrams in a full web give the extra contribution in question. The topological string partition functions of these sub-diagrams are then the extra contributions from the non-full spin content. Assuming the slicing invariance [37], the refined topological vertex formalism gives the following explicit expressions [27, 28]

$$Z^{\text{preferred}}_{\text{parallel } N-1 \text{ 5-branes}}(Q_1,\cdots,Q_N;t,q) = M(Q_1,\cdots,Q_N;t,q), \tag{4.2}$$

$$\begin{aligned} &Z^{\text{non-preferred}}_{\text{parallel } N-1 \text{ and } M-1 \text{ 5-branes}}(Q^u_1,\cdots,Q^u_N,Q^d_1,\cdots,Q^d_M;t,q) \\ &\qquad = \frac{M(Q^u_1,\cdots,Q^u_N;t,q)\,M(Q^d_M,\cdots,Q^d_1;q,t)}{M^{\text{pert.}}(Q^u_1,\cdots,Q^u_N,Q^d_1,\cdots,Q^d_M;t,q)}, \end{aligned} \tag{4.3}$$

$$M(Q_1,\cdots,Q_N;t,q) = \prod_{i,j=1}^{\infty}\prod_{1\le\ell\le m\le N}\frac{1}{1-Q_\ell Q_{\ell+1}\cdots Q_m\,t^i q^{j-1}}, \tag{4.4}$$

where $M^{\text{pert.}}(Q^u_1,\cdots,Q^u_N,Q^d_1,\cdots,Q^d_M;t,q)$ is the factors appearing in the numerator that are shared with the perturbative partition function of a full web diagram. This rule means that we do not take the finite legs that form the loop in this full web into consideration. We remove this factor $M^{\text{pert.}}$ because it can be collected into the perturbative part of the vector multiplet contribution that associated with the web loop.

Since these partition functions of the extra contributions are not invariant under the replacement of t with q, the corresponding spectrum does not form any representation of the little group of 5d Lorentz group $SU(2)_L \times SU(2)_R$. This means that the full spectrum contains extra states which do not form any full spin content of the Lorentz group.

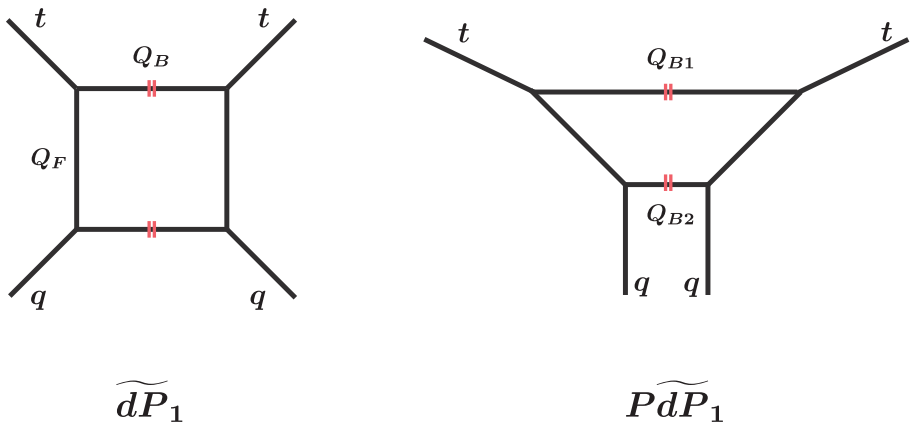

Figure 20: *The two toric diagrams associated with the* $\hat{\mathbf{E}}_1$ *configuration.*

To obtain proper spectrum in 5d, we have to remove such pathological contribution associated with a non-compact direction in the corresponding web configuration. This is the practical reason why we need to factor the non-full spin part out of a Nekrasov partition function.

4.1 The two toric phases for E_1 theory

Let us start with the simplest and non-trivial example. In the previous section, we claimed that the two Calabi-Yau manifolds $\widetilde{dP}_1$ and $P\widetilde{dP}_1$ lead to the same E_1 SCFT. We can check this claim by comparing their Nekrasov partition functions.

Since these two geometries share the same perturbative partition function, we compare their instanton partition functions. Using formulas in Appendix.B, we can compute the partition function of $\widetilde{dP}_1$

$$Z_{\widetilde{dP}_1}(u, Q_F; t, q) = \sum_{R_{1,2}} (-Q_B)^{|\vec{R}|} f_{R_1}^{-1}(t,q)\, f_{R_2}(t,q) K^{[\mathbf{1}]}_{R_1 R_2}(Q_F; t, q) K^{[\mathbf{1}]}_{R_2^T R_1^T}(Q_F; q, t), \quad (4.5)$$

where the instanton factor is $u = Q_B Q_F^{-1}$. The instanton part is then

$$Z^{\text{inst.}}_{\widetilde{dP}_1}(u, Q_F; t, q) = \sum_{R_{1,2}} \left(u \frac{q}{t}\right)^{|\vec{R}|} Z^{\text{vect.}}_{\vec{R}}(Q_F; t, q). \quad (4.6)$$

This is the Nekrasov instanton partition function of 5d $SU(2)$ pure Yang-Mills theory.

We can also compute the partition function of $P\widetilde{dP}_1$

$$
\begin{aligned}
&Z_{P\widetilde{dP}_1}(u, Q_F; t, q) \\
&= \sum_{R_{1,2}} (-Q_{B1})^{|R_1|} \, (-Q_{B2})^{|R_2|} \, f_{R_1}^{-3}(t,q) \, f_{R_2}^{-1}(t,q) K^{[\mathbf{1}]}_{R_1 R_2}(Q_F; t, q) K^{[\mathbf{1}]}_{R_2^T R_1^T}(Q_F; q, t),
\end{aligned} \tag{4.7}
$$

where the Kähler parameters associated with the base 2-cycle are

$$
Q_{B1} = u Q_F^2, \quad Q_{B1} = u. \tag{4.8}
$$

The instanton partition function is then

$$
Z^{\text{inst.}}_{P\widetilde{dP}_1}(u, Q_F; t, q) = \sum_{R_{1,2}} \left(u \frac{q}{t}\right)^{|\vec{R}|} Z^{\text{CS}, m=2}_{\vec{R}}(Q_F; t, q) \, Z^{\text{vect.}}_{\vec{R}}(Q_F; t, q). \tag{4.9}
$$

This is the Nekrasov instanton partition function of 5d $SU(2)$ Yang-Mills theory with the non-zero Cern-Simons level $m = 2$.

We can easily compute the one-instanton parts of these partition functions that are the terms proportional to u^1

$$
\begin{aligned}
Z^{\text{1-inst.}}_{\widetilde{dP}_1}(Q_F; t, q) &= \frac{q}{t} \frac{1 + \frac{q}{t}}{(1-q)(1-t^{-1})(1 - Q_F t^{-1} q)(1 - Q_F^{-1} t^{-1} q)}, \\
Z^{\text{1-inst.}}_{P\widetilde{dP}_1}(Q_F; t, q) &= \left(\frac{q}{t}\right)^2 \frac{Q_F + 1 + \frac{1}{Q_F} - \frac{q}{t}}{(1-q)(1-t^{-1})(1 - Q_F t^{-1} q)(1 - Q_F^{-1} t^{-1} q)}.
\end{aligned} \tag{4.10}
$$

They are obviously different rational functions. We, however, expect that the nontrivial relation (3.2) holds for them and there is certain simple connection between them. Remarkably, the Q_F-dependence disappears once one computes the difference

$$
Z^{\text{1-inst.}}_{\widetilde{dP}_1}(Q_F; t, q) - Z^{\text{1-inst.}}_{P\widetilde{dP}_1}(Q_F; t, q) = -\frac{q}{(1-q)(1-t)}. \tag{4.11}
$$

This term precisely cancels the contribution from the non-full spin content because the instanton expansion of the inversed extra contribution is

$$
\begin{aligned}
\frac{1}{Z_{\text{extra}}(u; q, t)} &= \prod_{i,j=1}^{\infty} (1 - u \, t^{i-1} q^j) \\
&= 1 - u \frac{q}{(1-q)(1-t)} + u^2 \frac{q^2(t+q)}{(1-q)^2(1-t)^2(1+q)(1+t)} + \cdots .
\end{aligned} \tag{4.12}
$$

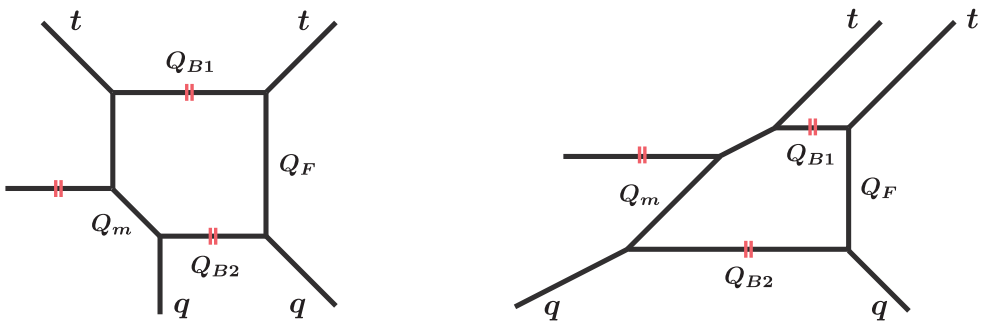

dP_2 PdP_2

Figure 21: *The two toric diagrams associated with the* $\hat{\mathbf{E}}_2$ *configuration.*

This result confirms the one-instanton part of the conjectural relation

$$Z^{\text{inst.}}_{\widetilde{dP}_1}(u, Q_F; t, q) = \frac{Z^{\text{inst.}}_{P\widetilde{dP}_1}(u, Q_F; t, q)}{Z_{\text{extra}}(u; q, t)}. \tag{4.13}$$

We can also prove it at the two-instanton level by showing the two-instanton part of the relation (3.2)

$$\begin{aligned} &Z^{\text{2-inst.}}_{\widetilde{dP}_1}(Q_F; t, q) - Z^{\text{2-inst.}}_{P\widetilde{dP}_1}(Q_F; t, q) \\ &= -\frac{q}{(1-q)(1-t)} Z^{\text{1-inst.}}_{P\widetilde{dP}_1}(Q_F; t, q) + \frac{q^2(t+q)}{(1-q)^2(1-t)^2(1+q)(1+t)}. \end{aligned} \tag{4.14}$$

The Q_F-dependence in the denominator is cancelled out again, and this difference in the two-instanton part can be collected into the expected extra factor (4.12). This test based on instanton expansion tells us that some unknown mathematical structure simplifies and factorizes the discrepancy between these two different partition functions.

4.2 The two toric phases for E_2 theory

As we showed in the previous section, there are two toric descriptions of the local del Pezzo dP_2. Since dP_2 is toric, we can compute its partition function directly by using the refined topological vertex formalism. The web-diagram of dP_2 is illustrated in the left hand side of ***Figure 21***, and this phase dP_2 was studied in [27, 28]. We review their

result for readers convenience. Its partition function is

$$Z_{dP_2}(u,Q_F,Q_m;t,q) = \sum_{R_{1,2}} (-Q_{B1})^{|R_1|}\,(-Q_{B2})^{|R_2|} \times f_{R_1}^{-1}(t,q)\, K^{[\mathbf{0},\mathbf{0}]}_{R_1R_2}(Q_F,Q_m;t,q) K^{[\mathbf{1}]}_{R_2^T R_1^T}(Q_F;q,t), \tag{4.15}$$

where the Kähler parameters for the base direction are

$$Q_{B1} = uQ_F, \quad Q_{B2} = \frac{uQ_F}{Q_m}. \tag{4.16}$$

The perturbative and instanton parts are therefore

$$Z^{\text{pert.}}_{dP_2}(u,Q_F,Q_m;t,q) = Z^{\text{vect.}}_{\text{pert.}}(Q_F;t,q) Z^{\text{matt.}}_{\text{pert.}}(Q_F,Q_m;t,q), \tag{4.17}$$

$$Z^{\text{inst.}}_{dP_2}(u,Q_F,Q_m;t,q) = \sum_{R_{1,2}} \left(u\frac{q}{t}\right)^{|\vec{R}|} Z^{\text{vect.}}_{\vec{R}}(Q_F;t,q) Z^{\text{matt.}}_{\vec{R}}(Q_F,Q_m;t,q). \tag{4.18}$$

The full partition function is the product of these two functions. This is the Nekrasov partition function of 5d $SU(2)$ gauge theory with single fundamental matter multiplet.

Pseudo del Pezzo Phase: PdP_2

We have the another description of the same system that is based on the pseudo del Pezzo PdP_2. The local pseudo del Pezzo surface PdP_2 is illustrated in the right hand side of ***Figure 21***, and its partition function is

$$Z_{PdP_2}(u,Q_F,Q_m;t,q) = \sum_{R_{1,2}} (-Q_{B1})^{|R_1|}\,(-Q_{B2})^{|R_2|} \times f_{R_1}(t,q)\, f^2_{R_2^T}(t,q) K^{[\mathbf{0},\mathbf{0}]}_{R_1R_2}(Q_F,Q_m;t,q) K^{[\mathbf{1}]}_{R_2^T R_1^T}(Q_F;q,t). \tag{4.19}$$

The Kähler parameters $Q_{B1,2}$ are

$$Q_{B1} = u, \quad Q_{B2} = \frac{uQ_F^2}{Q_m}. \tag{4.20}$$

The instanton part of this partition function takes the form

$$Z^{\text{inst.}}_{PdP_2}(u,Q_F,Q_m;t,q) = \sum_{R_{1,2}} \left(u\frac{q}{t}\right)^{|\vec{R}|} Z^{\text{CS},m=-2}_{\vec{R}}(Q_F;t,q) \times Z^{\text{vect.}}_{\vec{R}}(Q_F;t,q) Z^{\text{matt.}}_{\vec{R}}(Q_F,Q_m;t,q). \tag{4.21}$$

This web configuration contains the extra contribution that is raised from single stack of two parallel legs in ***Figure 21***

$$Z^{PdP_2}_{\text{extra}}(u;t,q) = M(u;t,q). \tag{4.22}$$

The partition function (4.21) is different from that of dP_2 (4.18) because this PdP_2 theory has the non-vanishing Chern-Simons level $m = 2$ as the case of $P\widetilde{dP}_1$.

Recall that branch cut move of the 7-brane configuration for $\hat{\mathbf{E}}_2$ leads to the following conjectural relation between these two descriptions

$$Z_{dP_2}(u, Q_F, Q_m; t, q) = \frac{Z^{\text{inst.}}_{PdP_2}(u, Q_F, Q_m; t, q)}{Z^{PdP_2}_{\text{extra}}(u; t, q)}. \tag{4.23}$$

Let us check this conjecture. Since the perturbative partition function is the same for these two phases, we need to check the instanton part of this relation. The one-instanton partition functions, which are the first order of u-expansion, are

$$\begin{aligned} Z^{\text{1-inst.}}_{dP_2} &= \frac{q}{t}\frac{1+\frac{q}{t}-\frac{1+Q_F}{Q_m}\sqrt{\frac{q}{t}}}{(1-q)(1-t^{-1})(1-Q_F t^{-1}q)(1-Q_F^{-1}t^{-1}q)}, \\ Z^{\text{1-inst.}}_{PdP_2} &= \frac{q}{t}\frac{Q_F+1+\frac{1}{Q_F}-\frac{t}{q}-\frac{1+Q_F}{Q_m}\sqrt{\frac{q}{t}}}{(1-q)(1-t^{-1})(1-Q_F t^{-1}q)(1-Q_F^{-1}t^{-1}q)}, \end{aligned} \tag{4.24}$$

and after computing the difference between them, dependence on Q_F and Q_m disappears

$$Z^{\text{1-inst.}}_{dP_2} - Z^{\text{1-inst.}}_{PdP_2} = -\frac{t}{(1-q)(1-t)}. \tag{4.25}$$

This is precisely the one-instanton part of the inversed extra factor $\frac{1}{Z^{PdP_2}_{\text{extra}}}$, and thus we can confirm our conjectural relation (4.23). Higher instanton check is also straightforward. We can check the two instanton part of the relation (4.23) for instance.

4.3 The four toric phases for E_3 theory

Let us move on to the case of the third del Pezzo. In this case we have four toric phases, where one of them is the toric local del Pezzo dP_3, and we expect the following relation

$$Z_{dP_3} = \frac{Z_{PdP_3^p}}{Z^{PdP_3^p}_{\text{extra}}}, \quad p = I,\ II,\ III. \tag{4.26}$$

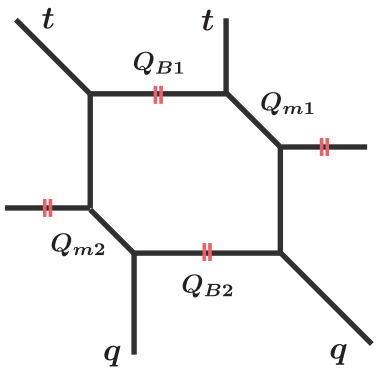

Figure 22: *The dP_3 toric diagram.*

The web diagram of dP_3 is given in ***Figure 22***. The refined topological vertex formalism gives to the following partition function of dP_3

$$\begin{aligned} &Z_{dP_3}(u, Q_F, Q_{m1,2}; t, q) \\ &= \sum_{R_{1,2}} (-Q_{B1})^{|R_1|} \, (-Q_{B2})^{|R_2|} \, K^{[\mathbf{0},\mathbf{0}]}_{R_1 R_2}(Q_F, Q_{m2}; t, q) K^{[\mathbf{0},\mathbf{0}]}_{R_2^T R_1^T}(Q_F, Q_{m1}; q, t), \end{aligned} \tag{4.27}$$

where the Kähler parameters for the base direction are

$$Q_{B1} = \frac{u Q_F}{Q_{m1}}, \quad Q_{B2} = \frac{u Q_F}{Q_{m2}}. \tag{4.28}$$

The perturbative and the instanton partition functions are therefore

$$Z_{dP_3}(Q_F, Q_{m1,2}; t, q) = Z^{\text{pert.}}_{dP_3}(Q_F, Q_{m1,2}; t, q) \, Z^{\text{inst.}}_{dP_3}(Q_F, Q_{m1,2}; t, q), \tag{4.29}$$

$$Z^{\text{pert.}}_{dP_3}(Q_F, Q_{m1,2}; t, q) = Z^{\text{vect.}}_{\text{pert.}}(Q_F; t, q) Z^{\text{matt.}}_{\text{pert.}}(Q_F, Q_{m1}; t, q) Z^{\text{matt.}}_{\text{pert.}}(Q_F, Q_{m2}; t, q), \tag{4.30}$$

$$\begin{aligned} Z^{\text{inst.}}_{dP_3}(u, Q_F, Q_{m1,2}; t, q) = &\sum_{R_{1,2}} \left(u \frac{q}{t}\right)^{|\vec{R}|} Z^{\text{vect.}}_{\vec{R}}(Q_F; t, q) \\ &\times Z'^{\text{matt.}}_{\vec{R}}(Q_F, Q_{m1}; t, q) Z^{\text{matt.}}_{\vec{R}}(Q_F, Q_{m2}; t, q). \end{aligned} \tag{4.31}$$

Let us compare this partition function with those of pseudo del Pezzo surfaces. In addition to the three phases of the pseudo del Pezzo surfaces PdP_3^p, we have double assignments of the preferred direction in the cases $p = I, II$. There are thus five patterns of topological string partition function, and we show that these partition functions lead to that of dP_3 through the relation (4.26).

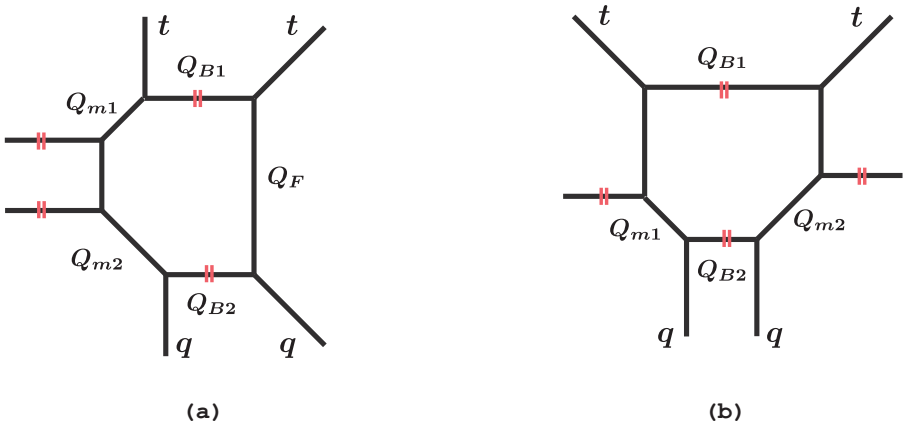

Figure 23: *The two choices of the preferred direction of the PdP_3^I toric diagram.*

Pseudo del Pezzo Phase I: PdP_3^I

The first phase PdP_3^I is illustrated in ***Figure 23***, and we can find two choices **(a,b)** of the preferred direction that is denoted by red double lines. This simple case PdP_3^I was already studied in [27, 28], but we review computation for readers convenience. These two choices **(a,b)** lead to different partition functions, however they reduce to the same dP_3 partition function after removing the extra contributions arising from their non-full spin contents. Let us star with the case **(a)**. The refined topological vertex formalism gives to the following partition function of $PdP_3^{I(a)}$

$$\begin{aligned} &Z_{PdP_3^{I(a)}}(u, Q_F, Q_{m1,2}; t, q) \\ &= \sum_{R_{1,2}} (-Q_{B1})^{|R_1|} (-Q_{B2})^{|R_2|} K_{R_1 R_2}^{[\mathbf{0},-\mathbf{1},\mathbf{0}]}(Q_F, Q_{m2}, Q_{m1}; t, q) K_{R_2^T R_1^T}^{[\mathbf{1}]}(Q_F; q, t), \end{aligned} \tag{4.32}$$

where the Kähler parameters $Q_{B1,2}$ are

$$Q_{B1} = \frac{u Q_F}{Q_{m1}}, \quad Q_{B2} = \frac{u Q_F}{Q_{m2}}. \tag{4.33}$$

Since the parallel external legs are horizontal, their contribution is independent of the instanton factor u. This extra factor therefore makes an effect only on the perturbative part, and the partition function is the product of the following perturbative and instanton

contributions

$$Z^{\text{pert.}}_{PdP_3^{I(a)}}(Q_F, Q_{m1,2}; t, q) = M\left(\frac{Q_F}{Q_{m1}Q_{m2}}; t, q\right) Z^{\text{pert.}}_{dP_3}(Q_F, Q_{m1,2}; t, q), \tag{4.34}$$

$$Z^{\text{inst.}}_{PdP_3^{I(a)}}(u, Q_F, Q_{m1,2}; t, q) = Z^{\text{inst.}}_{dP_3}(u, Q_F, Q_{m1,2}; t, q). \tag{4.35}$$

Because there is only single stack of parallel legs, the factor $M(Q_F(Q_{m1}Q_{m2})^{-1}; t, q)$ precisely gives the full extra contribution $Z^{PdP_3^{I(a)}}_{\text{extra}}$ coming from the non-full spin content. We can consequently prove the relation (4.26) for this case at all order in the instanton expansion.

The next case **(b)** comes with difficulty of proof of the relation because the extra factor involves u-dependence and it affects instanton expansion drastically. We will provide one-instanton check of the relation in the following. The partition function of **(b)** is

$$\begin{aligned} Z_{PdP_3^{I(b)}}(u, Q_F, Q_{m1,2}; t, q) = &\sum_{R_{1,2}} (-Q_{B1})^{|R_1|} \, (-Q_{B2})^{|R_2|} \, f_{R_1^T}(q, t) \, f_{R_2^T}(q, t) \\ &\times K^{[\mathbf{0},\mathbf{0}]}_{R_1 R_2}(Q_F, Q_{m1}; t, q) \, K^{[\mathbf{0},\mathbf{0}]}_{R_2^T R_1^T}(Q_F, \frac{Q_F}{Q_{m2}}; q, t), \end{aligned} \tag{4.36}$$

where the Kähler parameters $Q_{B1,2}$ are

$$Q_{B1} = uQ_F, \quad Q_{B2} = \frac{uQ_F}{Q_{m1}Q_{m2}}. \tag{4.37}$$

The perturbative partition function coincides with that of dP_3, but the instanton part takes the different form

$$Z^{\text{pert.}}_{PdP_3^{I(b)}}(Q_F, Q_{m1,2}; t, q) = Z^{\text{pert.}}_{dP_3}(Q_F, Q_{m1,2}; t, q) \tag{4.38}$$

$$\begin{aligned} &Z^{\text{inst.}}_{PdP_3^{I(b)}}(u, Q_F, Q_{m1,2}; t, q) \\ &= \sum_{R_{1,2}} \left(u\frac{q}{t}\right)^{|\vec{R}|} Z^{\text{vect.}}_{\vec{R}}(Q_F; t, q) Z^{\text{matt.}}_{\vec{R}}(Q_F, Q_{m1}; t, q) Z^{\text{matt.}}_{\vec{R}}(Q_F, Q_{m2}; t, q). \end{aligned} \tag{4.39}$$

Since the extra contribution arises from the downward parallel two legs in ***Figure 23***, its contribution is

$$Z^{PdP_3^{I(b)}}_{\text{extra}} = M(Q_{B2}; q, t), \tag{4.40}$$

and this function depends on u through Q_{B2}.

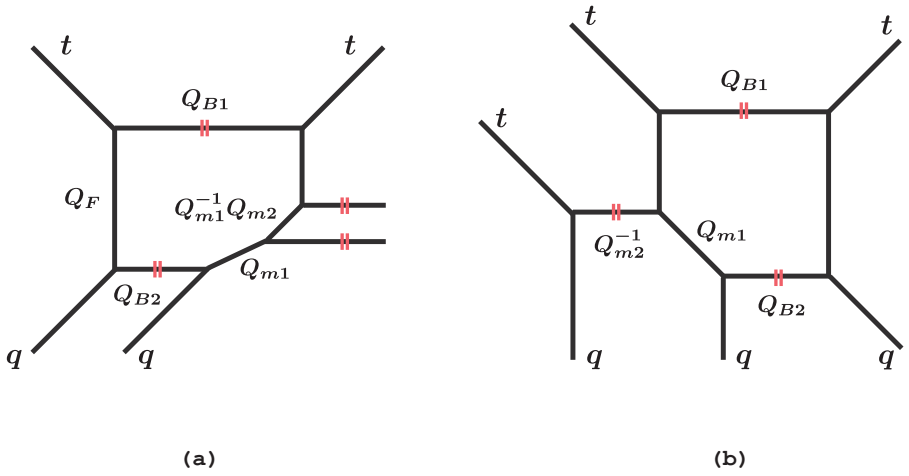

Figure 24: *The two choices of the preferred direction of the PdP_3^{II} toric diagram.*

It is straightforward to compute the one-instanton partition functions of $PdP_3^{I(a,b)}$ by using above results

$$\begin{aligned} &Z^{\text{1-inst.}}_{dP_3}(Q_F, Q_{m1,2}; t, q) = Z^{\text{1-inst.}}_{PdP_3^{I(a)}}(Q_F, Q_{m1,2}; t, q) \\ &= \frac{q}{t}\frac{\left(1+\frac{q}{t}\right)\left(1+\frac{Q_F}{Q_{m1}Q_{m2}}\right) - \left(\frac{1}{Q_{m1}}+\frac{1}{Q_{m2}}\right)(1+Q_F)\sqrt{\frac{q}{t}}}{(1-q)(1-t^{-1})(1-Q_F t^{-1}q)(1-Q_F^{-1}t^{-1}q)}, \end{aligned} \tag{4.41}$$

$$\begin{aligned} &Z^{\text{1-inst.}}_{PdP_3^{I(b)}}(Q_F, Q_{m1,2}; t, q) \\ &= \frac{q}{t}\frac{1+\frac{q}{t} - \left(\frac{1}{Q_{m1}}+\frac{1}{Q_{m2}}\right)(1+Q_F)\sqrt{\frac{q}{t}} + \frac{1}{Q_{m1}Q_{m2}}(Q_F^2+Q_F+1)\frac{q}{t} - \frac{Q_F}{Q_{m1}Q_{m2}}\left(\frac{q}{t}\right)^2}{(1-q)(1-t^{-1})(1-Q_F t^{-1}q)(1-Q_F^{-1}t^{-1}q)}. \end{aligned} \tag{4.42}$$

The difference between these partition functions is the following simple function

$$Z^{\text{1-inst.}}_{dP_3} - Z^{\text{1-inst.}}_{PdP_3^{I(b)}} = -\frac{Q_F}{Q_{m1}Q_{m2}}\frac{q}{(1-q)(1-t)}. \tag{4.43}$$

This is precisely the one-instanton part of our conjecture

$$Z_{dP_3} = \frac{Z_{PdP_3^{I(b)}}}{M\left(\frac{uQ_F}{Q_{m1}Q_{m2}}; q, t\right)}. \tag{4.44}$$

Pseudo del Pezzo Phase II: PdP_3^{II}

The second phase of PdP_3 has two choices of preferred direction, and these two cases are illustrated in ***Figure 24***. Since the diagrams **(a)** and **(b)** are related though $SL(2,\mathbb{Z})$ transformation and flop transition[5], these two setups describe the same toric manifold. We start with the case **(a)**. The refined topological vertex formalism yields the following expression

$$\begin{aligned} Z_{PdP_3^{II(a)}}(u, Q_F, Q_{m1,2}; t, q) = \sum_{R_{1,2}} (-Q_{B1})^{|R_1|} \, (-Q_{B2})^{|R_2|} \, f_{R_1}^{-1}(q,t) \, f_{R_2}^{-1}(q,t) \\ \times K^{[\mathbf{1}]}_{R_1 R_2}(Q_F; t, q) K^{[\mathbf{0},-\mathbf{1},\mathbf{0}]}_{R_2^T R_1^T} \left(Q_F, \frac{Q_F}{Q_{m2}}, Q_{m1}; q, t \right). \end{aligned} \tag{4.45}$$

The parameters $Q_{B1,2}$ are given by u as

$$Q_{B1} = u Q_F, \quad Q_{B2} = \frac{u Q_F}{Q_{m1} Q_{m2}}, \tag{4.46}$$

and then the partition function coming from two stacks takes the following form

$$\begin{aligned} Z_{PdP_3^{II(a)}} =& M\left(\frac{Q_{m2}}{Q_{m1}}; q, t\right) \, Z^{\text{vect}}_{\text{pert}}(Q_F) \, Z^{\text{matter}}_{\text{pert}}(Q_{m1}) \, Z^{\text{matter}}_{\text{pert}}(Q_{m2}) \\ & \times \sum_{R_{1,2}} \left(u \frac{q}{t}\right)^{|\vec{R}|} \, Z^{\text{vect.}}_{\vec{R}}(Q_F) \, Z^{\text{matt.}}_{\vec{R}}(Q_{m1}) \, Z^{\text{matt.}}_{\vec{R}}(Q_{m2}). \end{aligned} \tag{4.47}$$

Notice that the instanton part of this result is equal to (4.39). The extra contribution is given by

$$Z^{PdP_3^{II(a)}}_{\text{extra}} = M\left(\frac{Q_{m2}}{Q_{m1}}; q, t\right) \, M\left(\frac{u Q_F}{Q_{m1} Q_{m2}}; q, t\right), \tag{4.48}$$

and then we can show that this partition function is equivalent to that of $PdP_3^{I(b)}$ after removing the extra contributions as follows

$$\frac{Z_{PdP_3^{I(b)}}}{Z^{PdP_3^{I(b)}}_{\text{extra}}} = \frac{Z_{PdP_3^{II(a)}}}{Z^{PdP_3^{II(a)}}_{\text{extra}}}. \tag{4.49}$$

We therefore reduce the conjecture (4.26) in this case to that for the PdP_3^I phase (4.44).

Let us move on to the second choice of the preferred direction of PdP_3^{II} diagram that is illustrated in **(b)** of ***Figure 24***. This case is very non-trivial because the corresponding

[5]We employ the flop transition [46, 40] to avoid using the new vertex function [40].

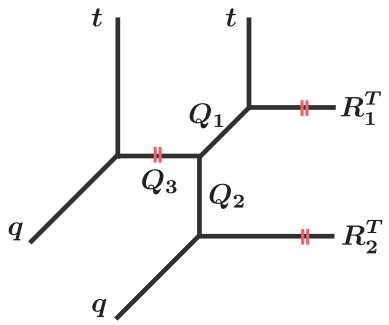

Figure 25: *The partition function of T^2 geometry with two non-empty Young diagrams on two adjoining external legs.*

topological string partition function is given by gluing a strip geometry [35] and the T^2 geometry which is a typical off-strip geometry ***Figure 25***. We therefore need to compute the topological string partition function of T^2 with two parallel external legs with non-empty Young diagrams. Unfortunately, it is very hard to compute exactly a partition function of such an off-strip geometry. This is because in this computation we confront certain summation over the Young diagrams that we can not evaluate by any combinatorial formula in existence. We hence compute this partition function up to certain order as a power series in a exponentiated Kähler parameter Q_3.

A noteworthy exception is the case with empty Young diagrams $R_1 = R_2 = \emptyset$ in ***Figure 25***, and we can find the following closed expression. The partition function in this case was recently computed in [27][6]

$$Z_{T^2}(Q_1,Q_2,Q_3,t,q) = \prod_{i,j=1}^{\infty} \frac{\left(1-Q_1Q_2Q_3t^{i-\frac{1}{2}}q^{j-\frac{1}{2}}\right)\prod_{\ell=1}^{3}\left(1-Q_\ell t^{i-\frac{1}{2}}q^{j-\frac{1}{2}}\right)}{\left(1-Q_1Q_2t^{i-1}q^j\right)\left(1-Q_2Q_3t^{i-1}q^j\right)\left(1-Q_1Q_3t^iq^{j-1}\right)}. \quad (4.50)$$

This closed expression was first observed in [47].

The topological string partition function with generic assignment of Young diagrams ***Figure 25*** is far more complicated. The topological vertex formalism yields

$$\begin{aligned} &K_{\vec{R}}^{T^2}(Q_1,Q_2,Q_3,t,q) \\ &= \sum_{Y_{1,2,3}} \prod_{\ell=1}^{3} (-Q_\ell)^{|Y_\ell|}\, C_{Y_1^T\emptyset R_1^T}(q,t)\, C_{\emptyset Y_2^T R_2^T}(q,t)\, C_{\emptyset\emptyset Y_3^T}(q,t)\, C_{Y_1Y_2Y_3}(t,q). \end{aligned} \quad (4.51)$$

[6]The unrefined version of T^2 partition function was computed in [48].

In contrast to the cases of strip geometries, there is no formulas to calculate all three summations over the Young diagrams $Y_{1,2,3}$. Using the Cauchy formulas reduces it to the following expression with a remaining summation over Y_3

$$K_{\vec{R}}^{T^2} = K_{\vec{R}}^{[\mathbf{1}]}(Q_1Q_2,t,q)\sum_{Y_3}(-Q_3)^{|Y_3|}\,t^{\frac{\|Y_3^T\|^2}{2}}q^{\frac{\|Y_3\|^2}{2}}\widetilde{Z}_{Y_3}(t,q)\,\widetilde{Z}_{Y_3^T}(q,t)$$
$$\times\prod_{i,j=1}^{\infty}\left(1-Q_1t^{-R_{1j}^T+i-\frac{1}{2}}q^{-Y_{3i}+j-\frac{1}{2}}\right)\left(1-Q_1t^{-Y_{3j}^T+i-\frac{1}{2}}q^{-R_{2i}+j-\frac{1}{2}}\right). \tag{4.52}$$

The extra contribution coming from non-full spin content on T^2 local geometry is included in the expression (4.50) as $M(Q_2Q_3;q,t)M(Q_1Q_3;t,q)$, and thus we normalize the partition function by this function Z_{T^2}. The topological string partition function is then

$$K_{\vec{R}}^{T^2}(Q_1,Q_2,Q_3,t,q)$$
$$=\frac{Z_{T^2}(Q_1,Q_2,Q_3,t,q)}{M(Q_1Q_2;q,t)}K_{\vec{R}}^{[\mathbf{1}]}(Q_1Q_2,t,q)P_{\vec{R}}(Q_1,Q_2,Q_3,t,q). \tag{4.53}$$

The remarkable characteristics of this function is that $P_{\vec{R}}(Q_1,Q_2,Q_3,t,q)$ is a polynomial in Q_3 even though this function is defined as a ratio of infinite power series in Q_3 as was first observed in [28, 27]. Let us consider simplest case $\vec{R}=([1],\emptyset)$

$$P_{([1],\emptyset)}(Q_1,Q_2,Q_3,t,q)=\frac{\prod_{i,j}\left(1-Q_2Q_3t^{i-1}q^j\right)\left(1-Q_1Q_3t^iq^{j-1}\right)}{\prod_{i,j}\left(1-Q_1Q_2Q_3t^{i-\frac{1}{2}}q^{j-\frac{1}{2}}\right)\left(1-Q_3t^{i-\frac{1}{2}}q^{j-\frac{1}{2}}\right)}$$
$$\times\sum_{Y}(-Q_3)^{|Y|}\,t^{\frac{\|Y^T\|^2}{2}}q^{\frac{\|Y\|^2}{2}}\widetilde{Z}_Y(t,q)\,\widetilde{Z}_{Y^T}(q,t)$$
$$\times\prod_{s\in Y}\left(1-Q_1t^{-\ell_{[1]}-\frac{1}{2}}q^{-a_Y-\frac{1}{2}}\right)\left(1-Q_2t^{\ell_\emptyset+\frac{1}{2}}q^{a_Y+\frac{1}{2}}\right)\prod_{s=(1,1)}\left(1-Q_1t^{\ell_Y+\frac{1}{2}}q^{a_{[1]}+\frac{1}{2}}\right). \tag{4.54}$$

Computing this summation up to few order in Q_3, we can confirm that this function is actually the following simple linear function of Q_3 because of certain cancellation mechanism

$$P_{([1],\emptyset)}(Q_1,Q_2,Q_3,t,q)=1-(Q_1+Q_1Q_2Q_3)\sqrt{\frac{q}{t}}+Q_1Q_3. \tag{4.55}$$

Using this result on T^2 partition function, we can compute the partition function of

$PdP_3^{II(b)}$. The refined topological vertex gives

$$Z_{PdP_3^{II(b)}} = \sum_{R_{1,2}} (-Q_{B1})^{|R_1|} (-Q_{B2})^{|R_2|} f_{R_1}^{-1}(t,q) \times K^{T^2}_{(R_1,R_2)}(Q_1,Q_2,Q_3,t,q)\, K^{[\mathbf{1}]}_{(R_2^T,R_1^T)}(Q_F,q,t). \tag{4.56}$$

We introduce the following parametrization

$$Q_F = Q_1 Q_2, \quad Q_2 = Q_{m1}, \quad Q_3 = \frac{1}{Q_{m2}}. \tag{4.57}$$

The partition function then takes the following form

$$Z_{PdP_3^{II(b)}} = M(Q_2Q_3;q,t)\, M(Q_1Q_3;t,q)\, Z^{\rm vect}_{\rm pert}(Q_F)\, Z^{\rm matter}_{\rm pert}(Q_{m1})\, Z^{\rm matter}_{\rm pert}(Q_{m2}) \times \sum_{R_{1,2}} \left(u\frac{q}{t}\right)^{|\vec{R}|} Z^{\rm vect}_{\vec{R}}(Q_F)(Q_{m1})^{-|R_2|}\, f_{R_2}^{-1}(t,q)\, P_{\vec{R}}(Q_{1,2,3};t,q). \tag{4.58}$$

Using (4.55) gives the following one-instanton partition function

$$Z^{\text{1-inst.}}_{PdP_3^{II(b)}} = \frac{q}{t} \frac{\left(1+\frac{q}{t}\right)\left(1+\frac{Q_F}{Q_{m1}Q_{m2}}\right) - \left(\frac{1}{Q_{m1}}+\frac{1}{Q_{m2}}\right)(1+Q_F)\sqrt{\frac{q}{t}}}{(1-q)(1-t^{-1})(1-Q_F t^{-1}q)(1-Q_F^{-1}t^{-1}q)} = Z^{\text{1-inst.}}_{dP_3}. \tag{4.59}$$

We can expect this equality is valid to all order in the instanton expansion of $Z^{\rm inst.}_{PdP_3^{II(b)}} = Z^{\rm inst.}_{dP_3}$. Moreover the extra contribution $M(Q_2Q_3;q,t)\, M(Q_1Q_3;t,q)$ does not make an effect on the instanton part. Therefore, this result provides one-instanton check of the relation

$$Z_{dP_3} = \frac{Z_{PdP_3^{II(b)}}}{Z^{PdP_3^{II(b)}}_{\rm extra}}. \tag{4.60}$$

Pseudo del Pezzo Phase III: PdP_3^{III}

The third phase is also nontrivial since it involves T^2 geometry as a toric sub-diagram. The web diagram and the assignment of the preferred direction are illustrated in ***Figure 26***. We can decompose the web into T^2 and a strip geometry in the right hand side. Gluing the topological string partition functions of the T^2 and strip sub-geometries yields the the partition function of PdP_3^{III}

$$Z_{PdP_3^{III}} = \sum_{R_{1,2}} (-Q_{B1})^{|R_1|} (-Q_{B2})^{|R_2|} f_{R_1}(t,q)\, \left(f_{R_2}(t,q)\right)^2 \times K^{T^2}_{(R_1,R_2)}(Q_F,Q_1,Q_2,Q_3,t,q)\, K^{[\mathbf{1}]}_{(R_2^T,R_1^T)}(Q_1Q_2,q,t). \tag{4.61}$$

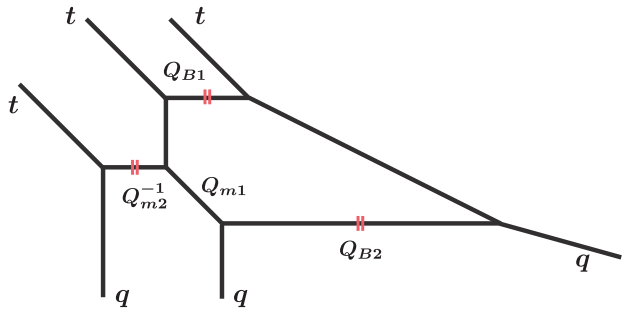

Figure 26: *The PdP_3^{III} toric diagram.*

The instanton factor u is given by

$$Q_{B1} = u, \quad Q_{B2} = uQ_1(Q_2)^2. \tag{4.62}$$

The partition function then takes the following form

$$\begin{aligned} Z_{PdP_3^{III}} &= M(Q_2Q_3;q,t)\, M(Q_1Q_3;t,q)\, Z^{\rm vect}_{\rm pert}(Q_1Q_2)\, Z^{\rm matter}_{\rm pert}(Q_2)\, Z^{\rm matter}_{\rm pert}(Q_3^{-1}) \\ &\times \sum_{R_{1,2}} \left(u\frac{q}{t}\right)^{|\vec{R}|}\, Z^{\rm vect}_{\vec{R}}(Q_1Q_2)(Q_1Q_2)^{-|R_1|}\,(Q_2)^{|R_2|}\, f^2_{R_1}(t,q)\, f_{R_2}(t,q)\, P_{\vec{R}}(Q_{1,2,3};t,q). \end{aligned} \tag{4.63}$$

Let us compare this result with the del Pezzo partition function. To ensure the coincidence between perturbative partition functions, the Coulomb branch and mass parameters in the Nekrasov partition function are introduced as

$$Q_F = Q_1Q_2, \quad Q_2 = Q_{m1}, \quad Q_3 = \frac{1}{Q_{m2}}. \tag{4.64}$$

Then the one instanton part is given by

$$Z^{\text{1-inst.}}_{PdP_3^{III}} = \frac{q}{t}\frac{\left(1+\frac{Q_F}{Q_{m1}Q_{m2}}\right)\left(-\frac{t}{q}+Q_F+1+\frac{1}{Q_F}\right)-\sqrt{\frac{q}{t}}\left(\frac{1}{Q_{m1}}+\frac{1}{Q_{m2}}\right)(1+Q_F)}{(1-q)(1-t^{-1})(1-Q_F^{-1}t^{-1}q)(1-Q_Ft^{-1}q)}. \tag{4.65}$$

It is easy to see that the difference between the following partition functions takes simple form

$$Z^{\text{1-inst.}}_{dP_3} - Z^{\text{1-inst.}}_{PdP_3^{III}} = -\left(1+\frac{Q_F}{Q_{m1}Q_{m2}}\right)\frac{t}{(1-q)(1-t)}. \tag{4.66}$$

This provides the one instanton confirmation of the expected relation

$$Z^{\text{inst.}}_{dP_3} = \frac{Z^{\text{inst.}}_{PdP_3^{III}}}{M(u;t,q)\, M\left(\frac{uQ_F}{Q_{m1}Q_{m2}};t,q\right)}. \tag{4.67}$$

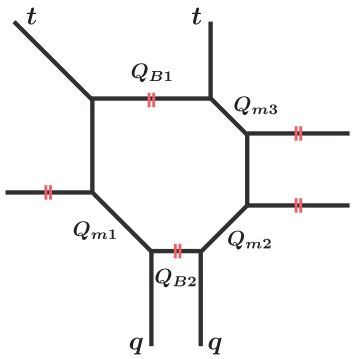

Figure 27: *The PdP_4^I toric diagram.*

Meanwhile it is easy to show that the perturbative part satisfies

$$Z^{\text{pert.}}_{dP_3} = \frac{Z^{\text{pert.}}_{PdP_3^{III}}}{M\left(\frac{Q_F}{Q_{m1}Q_{m2}};t,q\right)\, M\left(\frac{Q_{m1}}{Q_{m2}};q,t\right)}. \tag{4.68}$$

These results are consistent with our expression of the extra part of the partition function

$$Z^{PdP_3^{III}}_{\text{extra}} = M\left(\frac{Q_{m1}}{Q_{m2}};q,t\right)\, M\left(\frac{Q_F}{Q_{m1}Q_{m2}};t,q\right)\, M(u;t,q)\, M\left(\frac{uQ_F}{Q_{m1}Q_{m2}};t,q\right). \tag{4.69}$$

The relation (3.20) is consequently satisfied in one-instanton level.

4.4 The toric phases for E_4 theory

Since the local del Pezzo surface dP_4 is non-toric, we can not compute its partition function directly by using the refined topological vertex formalism. However we have two pseudo del Pezzo descriptions of dP_4, and we can expect that the dP_4 partition function coincides with those of toric PdP_4s after removing extra contribution.

Pseudo del Pezzo Phase I: PdP_4^I

The first phase PdP_4^I of dP_4 is illustrated in ***Figure 27***. This simple case was already studied in [27, 28], but we review computation for readers convenience. The gauge theory parameters are given by

$$Q_{B1} = \frac{uQ_F}{Q_{m3}}, \quad Q_{B2} = \frac{uQ_F}{Q_{m1}Q_{m2}}. \tag{4.70}$$

Using the refined topological vertex formalism gives the following expression of the PdP_4^I partition function

$$Z_{PdP_4^I} = \sum_{R_{1,2}} (-Q_{B1})^{|R_1|} (-Q_{B2})^{|R_2|} \left(f_{R_2}(t,q)\right)^{-1} \times K^{[\mathbf{0},-\mathbf{1}]}_{(R_1,R_2)}(Q_F, Q_{m1}; t, q)\, K^{[\mathbf{0},-\mathbf{1},\mathbf{0}]}_{(R_2^T,R_1^T)}(Q_F, Q_{m3}, Q_{m2}; q, t) = Z^{\text{pert.}}_{PdP_4^I}\, Z^{\text{inst.}}_{PdP_4^I}, \quad (4.71)$$

where the perturbative and instanton parts are

$$Z^{\text{pert.}}_{PdP_4^I} = M\left(\frac{Q_F}{Q_{m2}Q_{m3}}; q, t\right)\, Z^{\text{vect}}_{\text{pert}}(Q_F) \prod_{f=1}^{3} Z^{\text{matter}}_{\text{pert}}(Q_{mf}), \quad (4.72)$$

$$Z^{\text{inst.}}_{PdP_4^I} = \sum_{R_{1,2}} \left(u\frac{q}{t}\right)^{|\vec{R}|}\, Z^{\text{vect}}_{\vec{R}}(Q_F)\, Z^{\text{matt.}}_{\vec{R}}(Q_{m1})\, Z^{\text{matt.}}_{\vec{R}}(Q_{m2})\, Z'^{\text{matt.}}_{\vec{R}}(Q_{m3}). \quad (4.73)$$

The web of the toric geometry PdP_4^I has two stacks of two parallel external legs. The extra contribution thus takes the following form

$$Z^{PdP_4^I}_{\text{extra}} = M\left(\frac{uQ_F}{Q_{m1}Q_{m2}}; q, t\right)\, M\left(\frac{Q_F}{Q_{m2}Q_{m3}}; q, t\right). \quad (4.74)$$

Since the factor $M\left(Q_F/Q_{m2}Q_{m3}; t, q\right)$ appears in the overall coefficient and does not depend on the instanton factor u, we can recast our conjecture in terms of the instanton partition functions

$$Z^{\text{inst.}}_{dP_4} = \frac{Z^{\text{inst.}}_{PdP_4^I}}{M\left(\frac{uQ_F}{Q_{m1}Q_{m2}}; q, t\right)}. \quad (4.75)$$

This relation was checked in [27, 28] by comparing it with the Nekrasov partition function and the superconformal index of the corresponding $Sp(1)$ gauge theory [42] . In this article we employ an another point of view: this is not the unique topological string expression of the dP_4 partition function because there are other toric phases. We will compare the above partition function with those of other phases in the following. This computation provides an another check of our conjecture.

Pseudo del Pezzo Phase II: PdP_4^{II}

There are two choices of the preferred direction of the web-diagram of PdP_4^{II} as illustrated in ***Figure 28***. Let us start with the case of **(a)**. In this case the instanton factor given

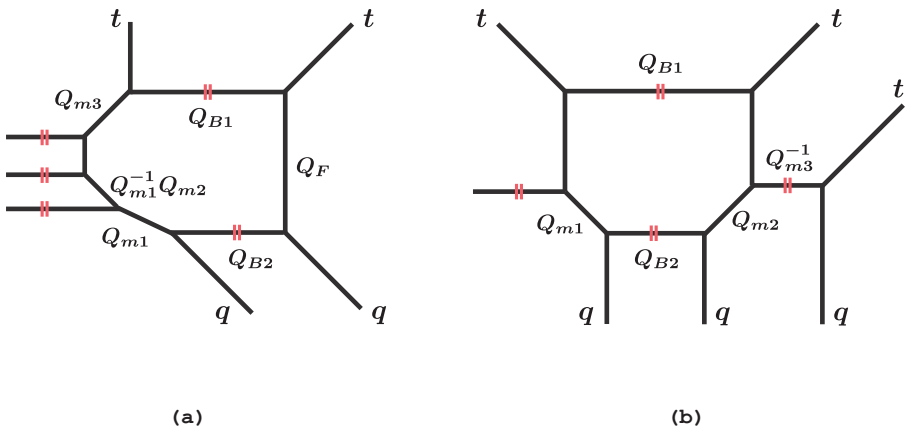

Figure 28: *The two choices of the preferred direction of the PdP_4^{II} toric diagram.*

by

$$Q_{B1} = \frac{uQ_F}{Q_{m3}}, \quad Q_{B2} = \frac{uQ_F}{Q_{m1}Q_{m2}}. \tag{4.76}$$

Applying the refined topological vergec formalism to this choice of the preferred direction yields the following expression

$$\begin{aligned} Z_{PdP_4^{II(a)}} &= \sum_{R_{1,2}} (-Q_{B1})^{|R_1|}(-Q_{B2})^{|R_2|} f_{R_1}^{-1}(t,q) \\ &\times K^{[\mathbf{0},\mathbf{-1},\mathbf{-1},\mathbf{0}]}_{(R_1,R_2)}(Q_F, Q_{m1}, Q_{m2}, Q_{m3}; t, q)\, K^{[\mathbf{1}]}_{(R_2^T,R_1^T)}(Q_F; q, t) = Z^{\text{pert.}}_{PdP_4^{II(a)}}\, Z^{\text{inst.}}_{PdP_4^{II(a)}}, \end{aligned} \tag{4.77}$$

and we can easily show

$$Z^{\text{pert.}}_{PdP_4^{II(a)}} = M\left(\frac{Q_F}{Q_{m2}Q_{m3}}, \frac{Q_F}{Q_{m1}Q_{m3}}; t, q\right) Z^{\text{vect}}_{\text{pert}}(Q_F) \prod_{f=1}^{3} Z^{\text{matter}}_{\text{pert}}(Q_{mf}), \tag{4.78}$$

$$Z^{\text{inst.}}_{PdP_4^{II(a)}} = Z^{\text{inst.}}_{PdP_4^{I}}. \tag{4.79}$$

Since the stacks of parallel external legs lead to the extra contribution

$$Z^{PdP_4^{II(a)}}_{\text{extra}} = M\left(\frac{Q_F}{Q_{m2}Q_{m3}}, \frac{Q_F}{Q_{m1}Q_{m3}}; t, q\right) M\left(\frac{uQ_F}{Q_{m1}Q_{m2}}; t, q\right), \tag{4.80}$$

we obtain the following relation

$$\frac{Z_{PdP_4^I}}{Z^{PdP_4^I}_{\text{extra}}} = \frac{Z_{PdP_4^{II(a)}}}{Z^{PdP_4^{II(a)}}_{\text{extra}}}. \tag{4.81}$$

Assuming the relation (4.75), we can thus prove our conjecture for $PdP_4^{II(a)}$ in all order in the instanton expansion.

The second case **(b)** in ***Figure 28*** is subtle because it involves the T^2 geometry. The instanton factor u given by

$$Q_{B1} = uQ_F, \quad Q_{B2} = \frac{uQ_F}{Q_{m1}Q_{m2}}, \tag{4.82}$$

and the topological string partition function is

$$\begin{aligned} Z_{PdP_4^{II(b)}} &= \sum_{R_{1,2}} (-Q_{B1})^{|R_1|} (-Q_{B2})^{|R_2|} f_{R_1}^{-1}(t,q)\, f_{R_2}^{-1}(t,q) \\ &\times K^{[\mathbf{0},-\mathbf{1}]}_{(R_1,R_2)}(Q_F, Q_{m1}; t, q)\, K^{T^2}_{(R_2^T,R_1^T)}(Q_F, Q_{m2}, Q_F Q_{m2}^{-1}, Q_{m3}^{-1}; q, t) = Z^{\text{pert.}}_{PdP_4^{II(b)}}\, Z^{\text{inst.}}_{PdP_4^{II(b)}}, \end{aligned} \tag{4.83}$$

and we can show

$$\frac{Z^{\text{pert.}}_{PdP_4^{II(b)}}}{M\left(\frac{Q_F}{Q_{m2}Q_{m3}}; t, q\right) M\left(\frac{Q_{m2}}{Q_{m3}}; q, t\right)} = \frac{Z^{\text{pert.}}_{PdP_4^{I}}}{M\left(\frac{Q_F}{Q_{m2}Q_{m3}}; q, t\right)}, \tag{4.84}$$

$$\begin{aligned} Z^{\text{inst.}}_{PdP_4^{II(b)}} &= \sum_{R_{1,2}} \left(u\frac{q}{t}\right)^{|\vec{R}|} (Q_{m2})^{|R_2|}\, f_{R_2}^{-1}(t,q)\, Z^{\text{vect}}_{\vec{R}}(Q_F)\, Z^{\text{matt.}}_{\vec{R}}(Q_{m1}) \\ &\times P_{(R_2^T,R_1^T)}(Q_{m2}, Q_F Q_{m2}^{-1}, Q_{m3}^{-1}; q, t). \end{aligned} \tag{4.85}$$

Our conjecture is therefore the following relation between two instanton partition functions

$$Z^{\text{inst.}}_{dP_4} = \frac{Z^{\text{inst.}}_{PdP_4^{II(b)}}}{M\left(\frac{uQ_F}{Q_{m1}Q_{m2}}; q, t\right) M\left(\frac{uQ_F}{Q_{m1}Q_{m3}}; q, t\right)}. \tag{4.86}$$

In the next subsection we verify an extended version of this equation in one-instanton order.

4.5 The toric phases for E_5 theory

Since the local del Pezzo surface dP_5 is also non-toric, we can not apply the refined topological vertex formalism directly to compute its partition function. However, we found three toric descriptions as pseudo del Pezzo surfaces. In this subsection, we verify our conjecture that all these pseudo del Pezzo surfaces PdP_4 lead to the unique dP_4 partition function after removing extra contribution.

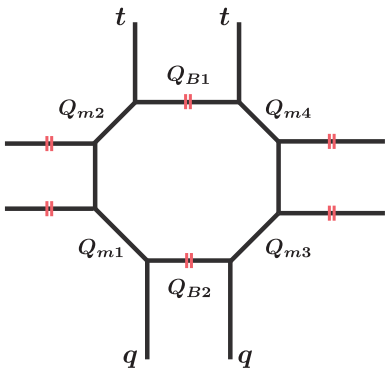

Figure 29: *The PdP_5^I toric diagram.*

Pseudo del Pezzo Phase I: PdP_5^I

We start with the simplest phase PdP_5^I. This case was already studied in [27, 28], and we review computation for readers convenience.

Using the refined topological vertex gives the PdP_5^I partition function

$$Z_{PdP_5^I} = \sum_{R_{1,2}} (-Q_{B1})^{|R_1|} (-Q_{B2})^{|R_2|} f_{R_1}(t,q)\, f_{R_2}^{-1}(t,q) K_{(R_1,R_2)}^{[\mathbf{0},\mathbf{-1},\mathbf{0}]}(Q_F, Q_{m1}, Q_{m2}; t, q)$$
$$\times K_{(R_2^T,R_1^T)}^{[\mathbf{0},\mathbf{-1},\mathbf{0}]}(Q_F, Q_{m4}, Q_{m3}; q, t) = Z_{PdP_5^I}^{\text{pert.}}\, Z_{PdP_5^I}^{\text{inst.}}, \tag{4.87}$$

where the instanton factor is given by

$$Q_{B1} = \frac{uQ_F}{Q_{m2}Q_{m4}}, \quad Q_{B2} = \frac{uQ_F}{Q_{m1}Q_{m3}}. \tag{4.88}$$

The perturbative and instanton partition functions are then given by

$$Z_{PdP_5^I}^{\text{pert.}} = M\left(\frac{Q_F}{Q_{m1}Q_{m2}}; t, q\right) M\left(\frac{Q_F}{Q_{m3}Q_{m4}}; q, t\right) Z_{\text{pert}}^{\text{vect}}(Q_F) \prod_{f=1}^{4} Z_{\text{pert}}^{\text{matter}}(Q_{mf}), \tag{4.89}$$

$$Z_{PdP_5^I}^{\text{inst.}}$$
$$= \sum_{R_{1,2}} \left(u\frac{q}{t}\right)^{|\vec{R}|} Z_{\vec{R}}^{\text{vect}}(Q_F)\, Z_{\vec{R}}^{\text{matt.}}(Q_{m1})\, Z_{\vec{R}}^{\text{matt.}}(Q_{m3})\, Z_{\vec{R}}^{\prime\text{matt.}}(Q_{m2})\, Z_{\vec{R}}^{\prime\text{matt.}}(Q_{m4}). \tag{4.90}$$

We can see that this instanton partition function is an asymmetric function of the mass parameters $Q_{m1,\cdots,4}$. Therefore, this partition function can not be that of dP_5 because dP_5 should have the symmetry with respect to the permutations of the mass parameters associated with the E_5 symmetry. This asymmetry is actually caused by the extra

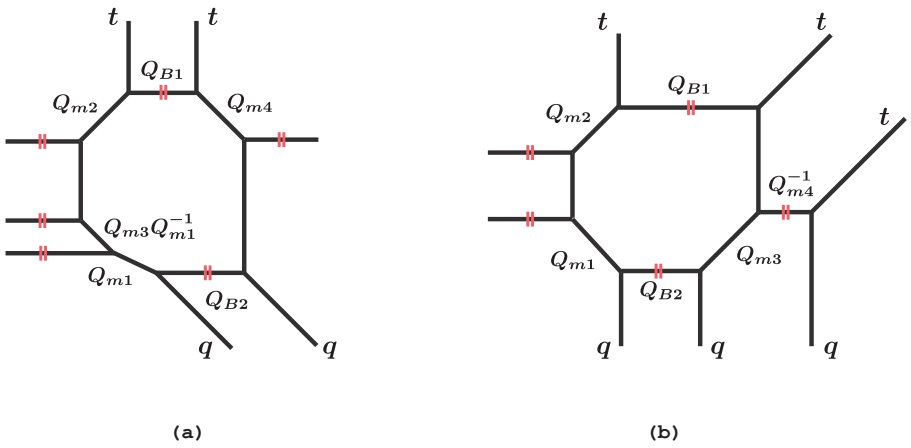

Figure 30: *The two choices of the preferred direction of the PdP_5^{II} toric diagram.*

contribution coming from four stacks in PdP_5^I geometry

$$Z_{\text{extra.}}^{PdP_5^I} = M\left(\frac{Q_F}{Q_{m1}Q_{m2}};t,q\right) M\left(\frac{Q_F}{Q_{m3}Q_{m4}};q,t\right) M\left(\frac{uQ_F}{Q_{m2}Q_{m4}};t,q\right) M\left(\frac{uQ_F}{Q_{m1}Q_{m3}};q,t\right), \quad (4.91)$$

and then we can expect that after the following renormalization of the instanton partition function it becomes a symmetric function of the mass parameters if our conjecture is valid

$$Z_{dP_5}^{\text{inst.}} = \frac{Z_{PdP_5^I}^{\text{inst.}}}{M\left(\frac{uQ_F}{Q_{m2}Q_{m4}};t,q\right) M\left(\frac{uQ_F}{Q_{m1}Q_{m3}};q,t\right)}. \quad (4.92)$$

In fact, we find that the one-instanton part of this renormalized partition function is

$$Z_{dP_5}^{\text{1-inst.}} = \frac{q}{t}\frac{\left(1+\frac{q}{t}\right)\left(1+\sum_{f_1\neq f_2}\frac{Q_F}{Q_{mf_1}Q_{mf_2}}+\frac{Q_F^2}{Q_{m1}Q_{m2}Q_{m3}Q_{m4}}\right)-\sqrt{\frac{q}{t}}\sum_{f=1}^4\left(\frac{1}{Q_{mf}}+\frac{Q_{mf}Q_F}{\prod_{g=1}^4 Q_{mg}}\right)(1+Q_F)}{(1-q)(1-t^{-1})(1-Q_Ft^{-1}q)(1-Q_F^{-1}t^{-1}q)}, \quad (4.93)$$

and it is manifestly symmetric. This enhancement of symmetry is a non-trivial evidence of our conjecture (4.92).

Pseudo del Pezzo Phase II: PdP_5^{II}

There are two choices of the preferred direction of the web-diagram of PdP_5^{II} as illustrated in ***Figure 30***. It is easy to compute the partition function of the case **(a)**

$$Z_{PdP_5^{II(a)}} = \sum_{R_{1,2}} (-Q_{B1})^{|R_1|} (-Q_{B2})^{|R_2|} f_{R_1}(t,q)\, f_{R_2}^{-1}(t,q)\, K_{(R_1,R_2)}^{[\mathbf{0},-\mathbf{1},-\mathbf{1},\mathbf{0}]}(Q_F, Q_{m1}, Q_{m3}, Q_{m2}; t, q)$$
$$\times K_{(R_2^T,R_1^T)}^{[\mathbf{0},\mathbf{0}]}(Q_F, Q_F Q_{m4}^{-1}; q, t) = Z_{PdP_5^I}^{\text{pert.}}\, Z_{PdP_5^I}^{\text{inst.}}. \tag{4.94}$$

The instanton factor u is given by the equations (4.88). The partition function then takes the following form

$$Z_{PdP_5^{II(a)}}^{\text{pert.}} = M\left(\frac{Q_F}{Q_{m2}Q_{m3}}, \frac{Q_{m3}}{Q_{m1}}; t, q\right) Z_{\text{pert}}^{\text{vect}}(Q_F) \prod_{f=1}^{4} Z_{\text{pert}}^{\text{matter}}(Q_{mf}), \tag{4.95}$$

$$Z_{PdP_5^{II(a)}}^{\text{inst.}} = Z_{PdP_5^I}^{\text{inst.}}, \tag{4.96}$$

and our factorization conjecture (3.33) actually holds for the extra contribution

$$Z_{\text{extra.}}^{PdP_5^{II(a)}} = M\left(\frac{Q_F}{Q_{m2}Q_{m3}}, \frac{Q_{m3}}{Q_{m1}}; t, q\right) M\left(\frac{uQ_F}{Q_{m2}Q_{m4}}; t, q\right) M\left(\frac{uQ_F}{Q_{m1}Q_{m3}}; q, t\right). \tag{4.97}$$

This extra factor is actually associated with the three stacks of external legs in the PdP_5^{II} web-diagram.

The partition function in the second case **(b)** contains the T^2 sub-diagram and its computation is more complicated. Using the refined topological vertex gives

$$Z_{PdP_5^{II(b)}} = \sum_{R_{1,2}} (-Q_{B1})^{|R_1|} (-Q_{B2})^{|R_2|}\, f_{R_2}^{-1}(t,q) K_{R_1,R_2}^{[\mathbf{0},-\mathbf{1},\mathbf{0}]}(Q_F, Q_{m1}, Q_{m2}; t, q)$$
$$\times K_{R_2^T,R_1^T}^{T^2}(Q_F, Q_{m3}, Q_F Q_{m3}^{-1}, Q_{m4}^{-1}, q, t), \tag{4.98}$$

where the Kähler parameters of the base 2-cycles are given by the instanton factor as

$$Q_{B1} = \frac{uQ_F}{Q_{m2}}, \quad Q_{B2} = \frac{uQ_F}{Q_{m1}Q_{m3}}. \tag{4.99}$$

We then find the following expression

$$Z_{PdP_5^{II(b)}}^{\text{pert.}} = M\left(\frac{Q_{m3}}{Q_{m4}}; q, t\right) Z_{PdP_5^I}^{\text{pert.}}, \tag{4.100}$$

$$Z_{PdP_5^{II(b)}}^{\text{inst.}} = \sum_{R_{1,2}} \left(u\frac{q}{t}\right)^{|\vec{R}|} (Q_{m3})^{|R_2|}\, f_{R_2}^{-1}(t,q)\, Z_{\vec{R}}^{\text{vect}}(Q_F)\, Z_{\vec{R}}^{\text{matt.}}(Q_{m1})\, Z'^{\text{matt.}}_{\vec{R}}(Q_{m2})$$
$$\times P_{R_2^T,R_1^T}(Q_{m3}, Q_F Q_{m3}^{-1}, Q_{m4}^{-1}, q, t). \tag{4.101}$$

Using (4.55), we obtain the one instanton part of this partition function

$$Z^{\text{1-inst.}}_{PdP_5^{II(b)}} = \frac{q}{t}\frac{N(Q_F, Q_{m1,2,3,4}; t, q)}{(1-q)(1-t^{-1})(1-Q_F t^{-1}q)(1-Q_F^{-1}t^{-1}q)}, \tag{4.102}$$

where the numerator is

$$\begin{aligned} N(Q_F, Q_{m1,2,3,4}; t, q) &= \left(1+\frac{q}{t}\right)\left(1+\frac{Q_F}{Q_{m1}Q_{m2}}+\frac{Q_F}{Q_{m3}Q_{m4}}+\frac{Q_F^2}{Q_{m1}Q_{m2}Q_{m3}Q_{m4}}\right) \\ &+\left(\frac{1}{Q_{m3}}+\frac{1}{Q_{m4}}\right)\left(\frac{q}{t}\frac{Q_F}{Q_{m1}}\left(-\frac{q}{t}+Q_F+1+\frac{1}{Q_F}\right)+\left(1+\frac{q}{t}\right)\frac{Q_F}{Q_{m2}}\right) \\ &-\sqrt{\frac{q}{t}}\sum_{f=1}^{4}\left(\frac{1}{Q_{mf}}+\frac{Q_{mf}Q_F}{\prod_{g=1}^{4}Q_{mg}}\right)(1+Q_F)\,. \end{aligned} \tag{4.103}$$

This partition function is not a symmetric function of $Q_{m1,2,3,4}$, and it does not coincide with the dP_5 partition function (4.93). The discrepancy in the one-instanton level, however, takes the following simple form

$$Z^{\text{1-inst.}}_{dP_5} - Z^{\text{1-inst.}}_{PdP_5^{II(b)}} = -\frac{q\left(\frac{Q_F}{Q_{m1}Q_{m3}}+\frac{Q_F}{Q_{m1}Q_{m4}}\right)}{(1-q)(1-t)}. \tag{4.104}$$

This precisely corresponds to the one-instanton part of the extra contribution

$$\begin{aligned} Z^{PdP_5^{II(b)}}_{\text{extra.}} &= M\left(\frac{Q_F}{Q_{m1}Q_{m2}};t,q\right)M\left(\frac{Q_F}{Q_{m3}Q_{m4}};t,q\right)\,M\left(\frac{Q_{m3}}{Q_{m4}};q,t\right) \\ &\quad\times M\left(\frac{uQ_F}{Q_{m1}Q_{m3}};q,t\right)\,M\left(\frac{uQ_F}{Q_{m1}Q_{m4}};q,t\right). \end{aligned} \tag{4.105}$$

This computation is therefore the one-instanton check of our conjecture (3.33).

Pseudo del Pezzo Phase III: PdP_5^{III}

The web-diagram of PdP_5^{II} also has two choices of the preferred direction as illustrated in ***Figure 31***. It is easy to compute the partition function of the first case **(a)**

$$\begin{aligned} Z_{PdP_5^{III(a)}} =& \sum_{R_{1,2}}(-Q_{B1})^{|R_1|}(-Q_{B2})^{|R_2|}f_{R_1}(t,q)\,f_{R_2}^{-1}(t,q) \\ &\times K^{[\mathbf{0},\mathbf{-1},\mathbf{-1},\mathbf{-1},\mathbf{0}]}_{(R_1,R_2)}(Q_F,Q_{m1},Q_{m3},Q_{m4},Q_{m2};t,q)\,K^{[\mathbf{1}]}_{(R_2^T,R_1^T)}(Q_F;q,t). \end{aligned} \tag{4.106}$$

Using (4.92) and some formulas in Appendix.B, we can easily show

$$Z^{\text{inst.}}_{dP_5} = \frac{Z^{\text{inst.}}_{PdP_5^{III(a)}}}{M\left(\frac{uQ_F}{Q_{m2}Q_{m4}};t,q\right)\,M\left(\frac{uQ_F}{Q_{m1}Q_{m3}};q,t\right)}, \tag{4.107}$$

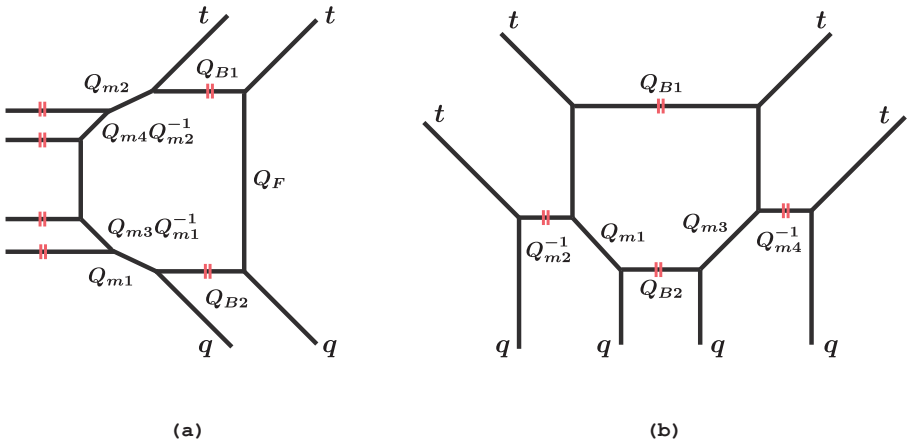

Figure 31: *The two choices of the preferred direction of the PdP_5^{III} toric diagram.*

and this partition function actually satisfies the relation (3.36). The extra contribution in this phase is given by

$$Z_{\text{extra.}}^{PdP_5^{III(a)}} = M\left(\frac{Q_{m4}}{Q_{m2}}, \frac{Q_F}{Q_{m3}Q_{m4}}, \frac{Q_{m3}}{Q_{m1}}; t, q\right) M\left(\frac{uQ_F}{Q_{m2}Q_{m4}}; t, q\right) M\left(\frac{uQ_F}{Q_{m1}Q_{m3}}; q, t\right). \quad (4.108)$$

This extra factor is actually associated with the three stacks of external legs in the PdP_5^{III} web-diagram.

The second case **(b)** of the third phase is the most non-trivial case in the pseudo fifth del Pezzo surfaces. This toric geometry is decomposed into two T^2 geometries as ***Figure 31***. The topological string partition function is

$$\begin{aligned} Z_{PdP_5^{III}} = & \sum_{R_{1,2}} (-Q_{B1})^{|R_1|} (-Q_{B2})^{|R_2|} f_{R_1}^{-1}(t,q)\, f_{R_2}^{-1}(t,q) \\ & \times K^{T^2}_{(R_1,R_2)}(Q_F, Q_1, Q_2, Q_3, t, q)\, K^{T^2}_{(R_2^T,R_1^T)}(Q_F, Q_1', Q_2', Q_3', q, t), \end{aligned} \quad (4.109)$$

where the gauge theory parameters are introduced by

$$Q_{B1} = uQ_F, \quad Q_{B2} = \frac{uQ_F}{Q_2 Q_1'}, \quad Q_F = Q_1 Q_2 = Q_1' Q_2', \quad (4.110)$$

$$Q_2 = Q_{m1}, \quad Q_3 = \frac{1}{Q_{m2}}, \quad Q_1' = Q_{m3}, \quad Q_3' = \frac{1}{Q_{m4}}. \quad (4.111)$$

Using (4.53) gives the following expression

$$
\begin{aligned}
Z_{PdP_5^{III(b)}} &= M(Q_2Q_3;q,t)\, M(Q_1Q_3;t,q)\, M(Q_2'Q_3';q,t)\, M(Q_1'Q_3';t,q) \\
&\times Z^{\rm vect}_{\rm pert}(Q_1Q_2) \prod_{f=1}^{4} Z^{\rm matter}_{\rm pert}(Q_{mf}) \sum_{R_{1,2}} \left(u\frac{q}{t}\right)^{|\vec{R}|}\, Z^{\rm vect}_{\vec{R}}(Q_1Q_2)\, (Q_2Q_1')^{-|R_2|} \\
&\times f_{R_2}^{-2}(t,q)\, P_{R_1,R_2}(Q_1,Q_2,Q_3;t,q) P_{R_2^T,R_1^T}(Q_1',Q_2',Q_3';q,t). \qquad (4.112)
\end{aligned}
$$

The first line $M(Q_2Q_3;q,t)\, M(Q_1Q_3;t,q)\, M(Q_2'Q_3';q,t)\, M(Q_1'Q_3';t,q) \equiv Z^{PdP_5^{III}}_{\rm extra,\,pert.}$ of this equation is the extra factor that does not depend on the instanton factor u. The remaining part of the extra contribution $Z^{PdP_5^{III(b)}}_{\rm extra} = Z^{PdP_5^{III(b)}}_{\rm extra,\,pert.} Z^{PdP_5^{III(b)}}_{\rm extra,\,inst.}$ is the following function

$$
\begin{aligned}
&Z^{PdP_5^{III(b)}}_{\rm extra,\,inst.} \\
&\equiv M\left(\frac{uQ_F}{Q_{m1}Q_{m3}};q,t\right)\, M\left(\frac{uQ_F}{Q_{m2}Q_{m3}};q,t\right)\, M\left(\frac{uQ_F}{Q_{m1}Q_{m4}};q,t\right)\, M\left(\frac{uQ_F}{Q_{m2}Q_{m4}};q,t\right). \qquad (4.113)
\end{aligned}
$$

To check our conjecture (3.36), let us compute the one-instanton part of the $Z_{PdP_5^{III(b)}}$ partition function. Using (4.55), we obtain

$$
Z^{\text{1-inst.}}_{PdP_5^{III(b)}} = \frac{q}{t}\frac{N(Q_F,Q_{m1,2,3,4};t,q)}{(1-q)(1-t^{-1})(1-Q_Ft^{-1}q)(1-Q_F^{-1}t^{-1}q)}, \qquad (4.114)
$$

where the numerator is

$$
\begin{aligned}
N(Q_F,Q_{m1,2,3,4};t,q) &= \left(1+\frac{q}{t}\right)\left(1+\frac{Q_F}{Q_{m1}Q_{m2}}+\frac{Q_F}{Q_{m3}Q_{m4}}+\frac{Q_F^2}{Q_{m1}Q_{m2}Q_{m3}Q_{m4}}\right) \\
&+\frac{q}{t}\left(-\frac{q}{t}+Q_F+1+\frac{1}{Q_F}\right)\left(\frac{Q_F}{Q_{m1}Q_{m3}}+\frac{Q_F}{Q_{m2}Q_{m3}}+\frac{Q_F}{Q_{m1}Q_{m4}}+\frac{Q_F}{Q_{m2}Q_{m4}}\right) \\
&-\sqrt{\frac{q}{t}}\sum_{f=1}^{4}\left(\frac{1}{Q_{mf}}+\frac{Q_{mf}Q_F}{\prod_{g=1}^{4}Q_{mg}}\right)(1+Q_F)\,. \qquad (4.115)
\end{aligned}
$$

This partition function is not a symmetric function of $Q_{m1,2,3,4}$. We can, however, show that the difference between this partition function and the symmetric one (4.93) of dP_5 takes the following simple form

$$
Z^{\text{1-inst.}}_{dP_5} - Z^{\text{1-inst.}}_{PdP_5^{III(b)}} = -\frac{q}{t}\frac{\frac{Q_F}{Q_{m1}Q_{m3}}+\frac{Q_F}{Q_{m2}Q_{m3}}+\frac{Q_F}{Q_{m1}Q_{m4}}+\frac{Q_F}{Q_{m2}Q_{m4}}}{(1-q)(1-t)}. \qquad (4.116)
$$

This is precisely equal to the one-instanton part of the extra factor (4.113). The relation (3.36) at the one-instanton level is thus satisfied through nontrivial cancellation between two rational functions $Z^{\text{1-inst.}}_{dP_5, PdP_5^{III(b)}}$. We expect such cancellation mechanism holds for all k-instanton partition functions.

5 Conclusion

In this paper, by extending the findings in [27, 28, 29], we have found duality between (p, q)-web configurations that lead to 5d field theories. This duality enables us to compute the topological string partition function of a (non-toric) local del Pezzo surface by employing a corresponding pseudo del Pezzo surface. In general, some pseudo del Pezzo surfaces are associated with a single del Pezzo surface.

There are sixteen inequivalent convex lattice polygons with single internal point, and this means that there are sixteen inequivalent 5-brane web configurations with single 5-brane loop. There are seemingly sixteen theories in 5d that arise from these configurations, however, we showed that some of these 5d theories are dual and there are only eight 5d theories. These eight theories are associated with the eight 5d SCFTs that have one dimensional Coulomb branch and flavor symmetry whose rank is less than 7. They were precisely the well-studied theories discovered by Seiberg in [1]. This means that no new theory appears because of the non-tivial duality between the corresponding Calabi-Yau singularities. This result provides the classification of the 5d SCFTs with one dimensional Coulomb branch that are associated with 5-brane web configurations. We can extend our discussion to web configurations with multiple 5-brane loops and classify the 5d SCFTs with higher dimensional Coulomb branch.

Our conjecture implies new mathematical relations between 5d $SU(2)$ Nekrasov partition functions. At first glance, two partition functions of different phases take very different combinatorial forms. Our conjecture, however, claims that the discrepancy between them can be collected into a simple prefactor. In this paper, we check this statement based on instanton expansion. It should be possible to verify our conjectural relations rigorously by employing and developing the mathematical theory of the Macdonald functions.

The 4d Seiberg duality observed in [17, 18, 19, 20, 21, 22, 23, 24, 25, 41] is deeply

related to our duality. In these papers, the authors considered quiver gauge theories that were the world-volume theories on D3-branes probing local del Pezzo singularities. Picking up some examples, they discussed that two theories are Seilerg-dual to each other if the corresponding toric singularities are related by 7-brane move for the corresponding 7-brane configurations. They considered the duality acting on the world-volume of probe D3-branes, but we can also consider the duality between the background singularities. This relation between toric singularities leads to our duality between 5d field theories. It would be interesting to study further relation between the 4d Seiberg-duality and our 5d analogous duality.

It would be also interesting if we can fine clear relation to the attempt at a non-toric extension of the topological vertex [57, 58] and the study on the E-string partition functions [59, 60].

Another unexplored line of research is the relation to the AGT conjecture [49, 50, 51, 52, 53]. The 5d version of the AGT conjecture [54, 55, 56, 27] recasts the 5d Nekrasov partition functions into the conformal blocks of the 2d q-deformed Toda field theories. Our relation between the topological string partition functions of the dual toric phases suggests that some 2d descriptions are associated to a single 5d theory. It would be interesting if we can find the role of the extra factors in the 2d side.

Acknowledgments

We are very grateful to Vladimir Mitev, Elli Pomoni and Futoshi Yagi for fruitful discussions and suggestions during collaborations.

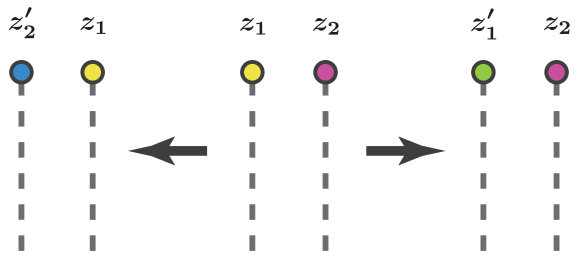

Figure 32: *The branch cut move of two adjoining 7-branes $\mathbf{X}_{z_{1,2}}$. By moving $\mathbf{X}_{z_2}$ across the branch cut of $\mathbf{X}_{z_1}$, the 7-brane charge z_2 changes into $z_2' = z_2 + (z_1 \wedge z_2)z_1$. Moving $\mathbf{X}_{z_1}$ yields the 7-brane with charge $z_1' = z_1 + (z_1 \wedge z_2)z_2$ on the right side.*

Appendix A : 7-branes and E_n symmetry

Recall that the $SL(2,\mathbb{Z})$ transformation of a D5-brane leads to the (p,q) 5-brane with generic NS-NS and Ramond-Ramond charges. Similarly, we can define the $[p,q]$ 7-brane as the $SL(2,\mathbb{Z})$ transformation of a D7-brane. The (p,q) 5-brane then can terminate on the $[p,q]$ 7-brane. The symbol $\mathbf{X}_{[p,q]}$ denotes the $[p,q]$ 7-brane. Notice that $\mathbf{X}_{[-p,-q]}$ is equivalent to $\mathbf{X}_{[p,q]}$.

We introduce the following three types of 7-branes for convenience sake

$$\mathbf{A}\text{-brane} : \mathbf{X}_{[1,0]} = \mathbf{A}, \quad \mathbf{B}\text{-brane} : \mathbf{X}_{[1,-1]} = \mathbf{B}, \quad \mathbf{C}\text{-brane} : \mathbf{X}_{[1,1]} = \mathbf{C}. \tag{5.1}$$

We also define the symplectic inner product between $[p,q]$ charges

$$z_i \equiv [p_i, q_i], \quad z_i \wedge z_j \equiv \det \begin{pmatrix} p_i & p_j \\ q_i & q_j \end{pmatrix}. \tag{5.2}$$

A 7-brane $\mathbf{X}_{[p,q]}$ creates a branch cut in the transversal plane, and the monodromy matrix around it is given by

$$K_{[p,q]} = \begin{pmatrix} 1+pq & -p^2 \\ q^2 & 1-pq \end{pmatrix} = 1 + zz^T S. \tag{5.3}$$

A.1 $SL(2,\mathbb{Z})$ transformation

$SL(2,\mathbb{Z})$ is generated by the two generators S and U, which are defined by

$$S = \begin{pmatrix} 0 & -1 \\ 1 & 0 \end{pmatrix}, \quad T = \begin{pmatrix} 1 & 0 \\ 1 & 1 \end{pmatrix}, \quad U = ST = \tag{5.4}$$

Type IIB superstring enjoys the $SL(2,\mathbb{Z})$ S-duality. The action of the duality change the dilaton and the axion as

$$SL(2,\mathbb{Z}) \ni \begin{pmatrix} a & b \\ c & d \end{pmatrix} \ : \ \tau \ \longmapsto \ \frac{a\tau + b}{c\tau + d}. \tag{5.5}$$

This also acts on the (p,q)-charges and the 7-brane monodormies as

$$SL(2,\mathbb{Z}) \ni g \ : \ \begin{pmatrix} p \\ q \end{pmatrix} \ \longmapsto \ g \begin{pmatrix} p \\ q \end{pmatrix}, \quad K_{[p,q]} \ \longmapsto \ g K_{[p,q]} g^{-1}. \tag{5.6}$$

A.2 7-brane move

Let us consider a 7-brane configuration $\mathbf{X}_{z_1}\mathbf{X}_{z_2}$. In our convention, the branch cuts go downward. We can consider two basic reordering procedure ***Figure 32***. When a 7-brane passes a branch cut, its charge chances with obeying the following rule

$$\mathbf{X}_{z_1}\mathbf{X}_{z_2} = \mathbf{X}_{z_2+(z_1\wedge z_2)z_1}\mathbf{X}_{z_1} = \mathbf{X}_{z_2}\mathbf{X}_{z_1+(z_1\wedge z_2)z_2}. \tag{5.7}$$

A.3 The collapsible 7-branes

The total monodromy $K = K_{z_n}\cdots K_{z_2}K_{z_1}$ around a collapsible 7-brane configuration satisfies the following condition

$$\mathrm{Tr}K = -2, -1, 0, 1, 2. \tag{5.8}$$

Appendix B : Nekrasov partition functions

B.1 The refined topological vertex

In this section, we collect definitions and conventions of the refined topological vertex formalism. The vertex function is

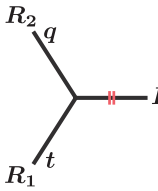

$$= C_{R_1R_2R_3}(t,q)$$

$$= (-1)^{|R_2|}\, f_{R_2^T}(t,q)\, q^{\frac{\|R_3\|^2}{2}}\, \tilde{Z}_{R_2}(t,q) \sum_Y S_{R_1^T/Y}(t^{-\rho}q^{R_3^T}) S_{R_2/Y}(q^{-\rho}t^{R_3}). \tag{5.9}$$

The leg marked with the red double line is the preferred direction. The framing factor is defined by

$$f_R(t,q) = (-1)^{|R|}\, t^{\frac{\|R^T\|^2}{2}}\, q^{-\frac{\|R\|^2}{2}}, \quad \widetilde{f}_R(t,q) = \left(\frac{t}{q}\right)^{\frac{|R|}{2}} f_R(t,q). \tag{5.10}$$

$\widetilde{Z}_R$ is the following specialized Macdonald function [61]

$$\widetilde{Z}_R(t,q) = \prod_{i=1}^{d(R)} \prod_{j=1}^{R_i} (1 - q^{R_i - j} t^{R_j^t - i + 1})^{-1}. \tag{5.11}$$

See [27] for the basic rules of the refined topological vertex formalism.

To compute topological string partition functions, we need to calculate summations of symmetric functions over the Young diagrams. The Cauchy formulas play a key role in this calculation

$$\sum_R S_{R/Y_1}(x)\, S_{R/Y_2}(y) = \prod_{i,j} (1 - x_i y_j)^{-1} \sum_R S_{Y_1/R}(y)\, S_{Y_2/R}(x), \tag{5.12}$$

$$\sum_R S_{R^T/Y_1}(x)\, S_{R/Y_2}(y) = \prod_{i,j} (1 + x_i y_j) \sum_R S_{Y_1^T/R}(y)\, S_{Y_2^T/R^T}(x). \tag{5.13}$$

B.2 $SU(2)$ Nekrasov partition functions

Let us introduce the following combinatorial factor

$$\begin{aligned} N_{R_\alpha R_\beta}(Q;t,q) &= \prod_{s \in R_\alpha} \left(1 - Q\, t^{\ell_{R_\beta}(s)} q^{a_{R_\alpha}(s)+1}\right) \prod_{t \in Y_\beta} \left(1 - Q\, t^{-(\ell_{R_\alpha}(t)+1)} q^{-a_{R_\beta}(t)}\right) \\ &= \prod_{i,j=1}^{\infty} \frac{1 - Q\, t^{-R^t_{\alpha,j}+i-1} q^{-R_{\beta,i}+j}}{1 - Q\, t^{i-1} q^j}. \end{aligned} \tag{5.14}$$

The $SU(2)$ vector multiplet contribution to the instanton part of the Nekrasov partition functions is

$$Z^{\text{vect.}}_{\vec{R}}(Q_{21};t,q) = \left(\frac{q}{t}\right)^{|\vec{R}|} \frac{1}{\prod_{\alpha,\beta=1,2} N_{R_\alpha R_\beta}(Q_{\beta\alpha};t,q)}, \tag{5.15}$$

where $Q_{\alpha\beta} = Q_\alpha Q_\beta^{-1}$, $Q_\alpha = e^{-R a_\alpha}$ and $a_1 = -a_2$. The contribution of the Chern-Simons term with the effective level m takes the following form [62]

$$Z^{\text{CS},m}_{\vec{R}}(Q_{21};t,q) = \prod_\alpha Q_\alpha^{-m|R_\alpha|} t^{-m\frac{\|R_\alpha^T\|^2}{2}} q^{m\frac{\|R_\alpha\|^2}{2}}. \tag{5.16}$$

The (anti)fundamental matter contribution is

$$Z^{\text{matt.}}_{\vec{R}}(Q_{21},Q_m;t,q)=\prod_{(i,j)\in R_1}\left(1-\frac{Q_{21}}{Q_m}\,t^{-i+\frac{1}{2}}q^{j-\frac{1}{2}}\right)\prod_{(i,j)\in R_2}\left(1-\frac{1}{Q_m}\,t^{-i+\frac{1}{2}}q^{j-\frac{1}{2}}\right), \tag{5.17}$$

$$Z'^{\text{matt.}}_{\vec{R}}(Q_{21},Q_m;t,q)=\prod_{(i,j)\in R_1}\left(1-\frac{1}{Q_m}\,t^{i-\frac{1}{2}}q^{-j+\frac{1}{2}}\right)\prod_{(i,j)\in R_2}\left(1-\frac{Q_{21}}{Q_m}\,t^{i-\frac{1}{2}}q^{-j+\frac{1}{2}}\right). \tag{5.18}$$

Notice that they satisfy

$$Z^{\text{matt.}}_{R_2^TR_1^T}(Q_{21},Q_m;q,t)=Z'^{\text{matt.}}_{R_1R_2}(Q_{21},Q_m;t,q). \tag{5.19}$$

We can also write down the perturbative contributions to the Nekrasov partition function. The vector multiplet contribution is

$$Z^{\text{vect.}}_{\text{pert.}}(Q_{21};t,q)=\prod_{i,j=1}^{\infty}\frac{1}{(1-Q_{21}t^{i-1}q^j)(1-Q_{21}t^iq^{j-1})}, \tag{5.20}$$

and the (anti)fundamental matter contribution is

$$Z^{\text{vect.}}_{\text{pert.}}(Q_{21},Q_m;t,q)=\prod_{i,j=1}^{\infty}\left(1-Q_mt^{i-\frac{1}{2}}q^{j-\frac{1}{2}}\right)\left(1-\frac{Q_{21}}{Q_m}t^{i-\frac{1}{2}}q^{j-\frac{1}{2}}\right). \tag{5.21}$$

The full Nekrasov partition function is then

$$\begin{aligned}&Z(Q_{21},u,Q_m;t,q)\\&=Z^{\text{vect.}}_{\text{pert}}(Q_{21};t,q)\prod_{\text{matters}}Z^{\text{matt.}}_{\text{pert}}(Q_{21},Q_m;t,q)\\&\times\sum_{\vec{R}}\left(u\frac{q}{t}\right)^{|\vec{R}|}Z^{\text{CS},m}_{\vec{R}}(Q_{21};t,q)Z^{\text{vect.}}_{\vec{R}}(Q_{21};t,q)\prod_{\text{matters}}Z^{\text{matt.}}_{\vec{R}}(Q_{21},Q_m;t,q),\end{aligned} \tag{5.22}$$

where m is the Chern-Simons level of this theory. The third line of this equation is the instanton partition function $Z^{\text{inst.}}$ of this theory, and we introduce the following instanton expansion

$$Z(Q_{21},u,Q_m;t,q)=1+\sum_{k=1}^{\infty}u^k\,Z^{k\text{-inst.}}(Q_{21},Q_m;t,q), \tag{5.23}$$

and $Z^{k\text{-inst.}}$ is the k-instanton partition function. In this paper, we use the following symbol to parametrize the Coulomb branch parameter

$$Q_F=Q_{21}. \tag{5.24}$$

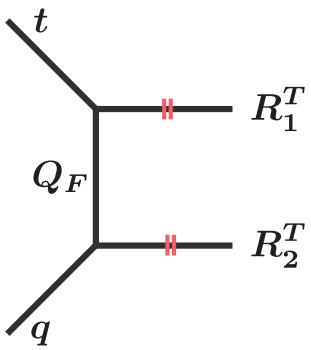

Figure 33: *A sub-diagram for $SU(2)$ geometry. We label this diagram by the framing number of the two-cycle Q_F as* $[\mathbf{1}]$.

B.3 Building blocks of Nekrasov partition functions

In this subsection, we compute building blocks of the topological string partition functions for the toric phases of the local del Pezzo surfaces $dP_{1,2,\cdots,6}$. ***Figure 33*** is the half geometry which gives the $\widetilde{dP_1}$ web diagram. The refined topological vertex on the geometry ***Figure 33*** gives the following partition function

$$\begin{aligned} K^{[\mathbf{1}]}_{R_1R_2}(Q_F;t,q) &= \sum_Y (-Q_F)^{|Y|}\, \tilde{f}_Y(q,t)\, C_{\emptyset Y R_1^T}(q,t)\, C_{Y^T \emptyset R_2^T}(q,t) \\ &= \prod_{\alpha=1,2} \left(t^{\frac{\|R_a^T\|}{2}} \tilde{Z}_{R_a^T}(q,t) \right) \frac{Z^{\text{vect.(L)}}_{\text{pert.}}(Q_F;t,q)}{N_{R_1R_2}(Q_F,t,q)}, \end{aligned} \tag{5.25}$$

where the perturbative part is defined by

$$Z^{\text{vect.(L)}}_{\text{pert}}(Q_F;t,q) = \prod_{i,j=1}^{\infty} (1 - Q_F t^{i-1} q^j)^{-1}. \tag{5.26}$$

The perturbative partition function of the vector multiplet is given by

$$Z^{\text{vect.}}_{\text{pert.}}(Q_F;t,q) = Z^{\text{vect.(L)}}_{\text{pert.}}(Q_F;t,q)\, Z^{\text{vect.(L)}}_{\text{pert.}}(Q_F;q,t). \tag{5.27}$$

We can show the following identity

$$\begin{aligned} &K^{[\mathbf{1}]}_{R_1R_2}(Q_F;t,q) K^{[\mathbf{1}]}_{R_2^T R_1^T}(Q_F;q,t) \\ &= Z^{\text{vect.}}_{\text{pert}}(Q_F;t,q) \left(-\frac{1}{Q_F} \frac{q}{t} \right)^{|\vec{R}|} f_{R_1}(t,q)\, f^{-1}_{R_2}(t,q) \prod_{\alpha,\beta=1,2} \frac{1}{N_{R_\alpha R_\beta}(Q_{\beta\alpha};t,q)}, \end{aligned} \tag{5.28}$$

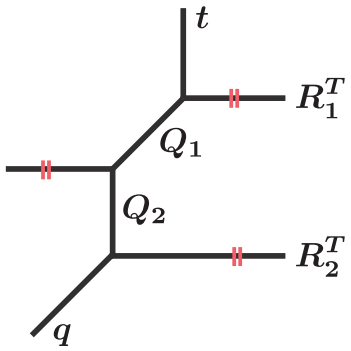

Figure 34: *A sub-diagram for $SU(2)$ geometry. We label this diagram by the framing numbers of the two-cycles as $[\mathbf{0},\mathbf{0}]$.*

which gives the $SU(2)$ vector multiplet contribution to the Nekrasov partition function. In our convention, the Coulomb branch parameter is given by $Q_{21} = Q_F$.

The sub-diagram ***Figure 34*** is used to construct the dP_2 geometry for instance. Using the refined topological vertex formalism gives

$$\begin{aligned} K^{[\mathbf{0},\mathbf{0}]}_{R_1R_2}(Q_1Q_2,Q_1;t,q) &= \sum_{Y_{1,2}} (-Q_1)^{|Y_1|}\,(-Q_2)^{|Y_2|}\; C_{Y_1^T\emptyset R_1^T}(q,t)\, C_{Y_1Y_2^T\emptyset}(t,q)\, C_{\emptyset Y_2R_2^T}(q,t) \\ &= K^{[\mathbf{1}]}_{R_1R_2}(Q_1Q_2;t,q) Z^{\text{matt.}}_{\text{pert.}}(Q_1Q_2,Q_1;t,q)\, Q_1^{|R_1|}\, f^{-1}_{R_1}(t,q) Z'^{\text{matt.}}_{\vec{R}}(Q_1Q_2,Q_1;t,q) \\ &= K^{[\mathbf{1}]}_{R_1R_2}(Q_1Q_2;t,q) Z^{\text{matt.}}_{\text{pert.}}(Q_1Q_2,Q_2;t,q)\, Q_2^{|R_1|}\, f_{R_2}(t,q) Z^{\text{matt.}}_{\vec{R}}(Q_1Q_2,Q_2;t,q). \end{aligned} \tag{5.29}$$

This local structure thus creates single matter multiplet whose mass is given by Q_2.

We come upon the geometry ***Figure 35*** in the computation of PdP_3 partition function. The refined topological vertex formalism leads to the following expression

$$\begin{aligned} & K^{[\mathbf{0},-\mathbf{1},\mathbf{0}]}_{R_1R_2}(Q_F,Q_3,Q_1;t,q) \\ &= \sum_{Y_{1,2,3}} (-Q_1)^{|Y_1|}\,(-Q_2)^{|Y_2|}\,(-Q_3)^{|Y_3|}\;\tilde{f}_{Y_2}(t,q) \\ &\times C_{Y_1^T\emptyset R_1^T}(q,t)\, C_{Y_1Y_2^T\emptyset}(t,q)\, C_{Y_2Y_3^T\emptyset}(t,q)\, C_{\emptyset Y_3R_2^T}(q,t) \\ &= M(Q_2;t,q) K^{[\mathbf{1}]}_{R_1R_2}(Q_F;t,q)\, Z^{\text{matt.}}_{\text{pert.}}(Q_F,Q_1;t,q)\, Z^{\text{matt.}}_{\text{pert.}}(Q_F,Q_3;t,q) \\ &\times Q_1^{|R_1|}Q_3^{|R_2|} f^{-1}_{R_1}(t,q) f_{R_2}(t,q) Z'^{\text{matt.}}_{\vec{R}}(Q_F,Q_1;t,q) Z^{\text{matt.}}_{\vec{R}}(Q_F,Q_3;t,q), \end{aligned} \tag{5.30}$$

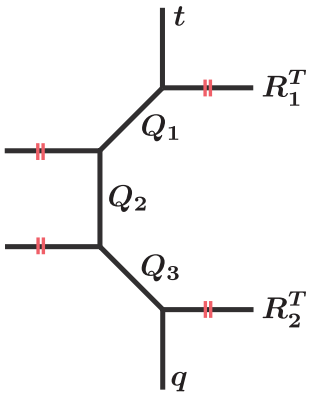

Figure 35: *The sub-diagram for $SU(2)$ geometry whose framing numbers of the two-cycles are $[\mathbf{0}, \mathbf{-1}, \mathbf{0}]$.*

where we introduce $Q_F = Q_1Q_2Q_3$. We can see that this local structure gives two matter multiplets.

The geometry ***Figure 36*** is used to compute PdP_4 partition function. By using the topological vertex, we obtain

$$\begin{aligned}
&K_{R_1R_2}^{[\mathbf{0},\mathbf{-1},\mathbf{-1},\mathbf{0}]}(Q_F, Q_5, Q_4Q_5, Q_1, Q_1Q_2; t, q) \\
&= \sum_{Y_{1,2,3,4}} (-Q_1)^{|Y_1|} (-Q_2)^{|Y_2|} (-Q_3)^{|Y_3|} (-Q_4)^{|Y_4|} \ \tilde{f}_{Y_2}(t,q)\tilde{f}_{Y_3}(t,q) \\
&\times C_{Y_1^T\emptyset R_1^T}(q,t)\, C_{Y_1Y_2^T\emptyset}(t,q)\, C_{Y_2Y_3^T\emptyset}(t,q)\, C_{Y_3Y_4^T\emptyset}(t,q)\, C_{\emptyset Y_4R_2^T}(q,t). \qquad (5.31)
\end{aligned}$$

With some algebra, we find the following expression

$$\begin{aligned}
&K_{R_1R_2}^{[\mathbf{0},\mathbf{-1},\mathbf{-1},\mathbf{0}]}(Q_F, Q_5, Q_4Q_5, Q_1, Q_1Q_2; t, q) = M(Q_2, Q_3; t, q) \prod_{Q_m = Q_{1,4}, Q_3Q_4} Z_{\text{pert.}}^{\text{matt.}}(Q_F, Q_m; t, q) \\
&\times Q_1^{|R_1|}(Q_3Q_4^2)^{|R_2|} f_{R_1}^{-1}(t,q) f_{R_2}^2(t,q)\, K_{R_1R_2}^{[\mathbf{1}]}(Q_F; t, q) \\
&\times Z'^{\text{matt.}}_{\vec{R}}(Q_F, Q_1; t, q) Z^{\text{matt.}}_{\vec{R}}(Q_F, Q_3Q_4; t, q) Z^{\text{matt.}}_{\vec{R}}(Q_F, Q_4; t, q), \qquad (5.32)
\end{aligned}$$

where we introduce $Q_F = Q_1Q_2Q_3Q_4$. Three matter multiplets are associated with this local structure.

The PdP_5^{III} diagram involves the sub-diagram ***Figure 37***. The refined topological

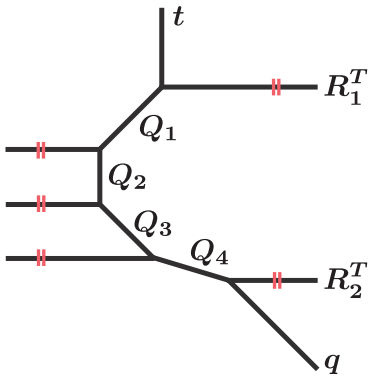

Figure 36: *A sub-diagram for $SU(2)$ geometry whose framing numbers of the two-cycles are* $[\mathbf{0}, \mathbf{-1}, \mathbf{-1}, \mathbf{0}]$.

vertex gives

$$
\begin{aligned}
&K_{R_1R_2}^{[\mathbf{0},\mathbf{-1},\mathbf{-1},\mathbf{-1},\mathbf{0}]}(Q_F, Q_4, Q_4Q_3, Q_1, Q_1Q_2; t, q) \\
&= \sum_{Y_{1,2,3,4,5}} (-Q_1)^{|Y_1|} (-Q_2)^{|Y_2|} (-Q_3)^{|Y_3|} (-Q_4)^{|Y_4|} (-Q_5)^{|Y_5|} \ \tilde{f}_{Y_2}(t,q)\tilde{f}_{Y_3}(t,q)\tilde{f}_{Y_4}(t,q) \\
&\times C_{Y_1^T\emptyset R_1^T}(q,t)\, C_{Y_1Y_2^T\emptyset}(t,q)\, C_{Y_2Y_3^T\emptyset}(t,q)\, C_{Y_3Y_4^T\emptyset}(t,q)\, C_{Y_4Y_5^T\emptyset}(t,q)\, C_{\emptyset Y_5 R_2^T}(q,t). \qquad (5.33)
\end{aligned}
$$

Using the Cauchy formulas, we obtain the following expression

$$
\begin{aligned}
K_{R_1R_2}^{[\mathbf{0},\mathbf{-1},\mathbf{-1},\mathbf{-1},\mathbf{0}]} &= M(Q_2, Q_3, Q_4; t, q) \prod_{Q_m = Q_{1,5}, Q_1Q_2, Q_4Q_5} Z_{\text{pert.}}^{\text{matt.}}(Q_F, Q_m; t, q) \\
&\times (Q_1^2Q_2)^{|R_1|}(Q_4Q_5^2)^{|R_2|} f_{R_1}^{-2}(t,q) f_{R_2}^2(t,q) K_{R_1R_2}^{[\mathbf{1}]}(Q_F; t, q)\, Z'^{\text{matt.}}_{\vec{R}}(Q_F, Q_1; t, q) \\
&\times Z'^{\text{matt.}}_{\vec{R}}(Q_F, Q_1Q_2; t, q) Z^{\text{matt.}}_{\vec{R}}(Q_F, Q_4Q_5; t, q) Z^{\text{matt.}}_{\vec{R}}(Q_F, Q_5; t, q), \qquad (5.34)
\end{aligned}
$$

where we introduce $Q_F = Q_1Q_2Q_3Q_4Q_5$. This local structure of a Calabi-Yau manifold leads to two fundamental matter multiplets and two anti-fundamental matter multiplets. We can therefore use this diagram to compute the partition function for E_5 SCFT.

T^2 subdiagram

In contrast, we can not give a closed expression of the T^2 sub-diagram ***Figure 25***. This is because the above cases are strip geometries [35, 38] whose partition functions are given

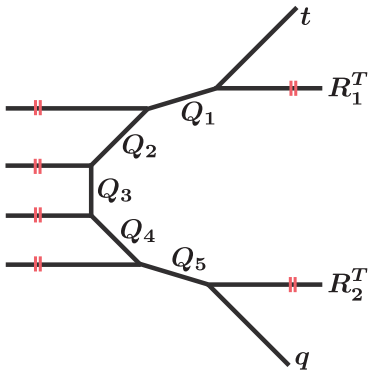

Figure 37: *A sub-diagram for $SU(2)$ geometry whose framing numbers of the two-cycles are* $[\mathbf{0}, \mathbf{-1}, \mathbf{-1}, \mathbf{-1}, \mathbf{0}]$.

by recursive applications of the Cauchy formulas. Using the topological vertex formalism yields the expression

$$\begin{aligned} & K_{\vec{R}}^{T^2}(Q_1, Q_2, Q_3, t, q) \\ & = \frac{Z_{T^2}(Q_1, Q_2, Q_3, t, q)}{M(Q_1 Q_2; q, t)} K_{\vec{R}}^{[\mathbf{1}]}(Q_1 Q_2, t, q) P_{\vec{R}}(Q_1, Q_2, Q_3, t, q), \end{aligned} \tag{5.35}$$

where

$$\begin{aligned} P_{\vec{R}}(Q_1, Q_2, Q_3, t, q) = & \frac{\prod_{i,j=1}^{\infty} \left(1 - Q_2 Q_3 t^{i-1} q^j\right) \left(1 - Q_1 Q_3 t^i q^{j-1}\right)}{\prod_{i,j=1}^{\infty} \left(1 - Q_1 Q_2 Q_3 t^{i-\frac{1}{2}} q^{j-\frac{1}{2}}\right) \left(1 - Q_3 t^{i-\frac{1}{2}} q^{j-\frac{1}{2}}\right)} \\ & \times \sum_Y (-Q_3)^{|Y|} t^{\frac{\|Y^T\|^2}{2}} q^{\frac{\|Y\|^2}{2}} \widetilde{Z}_Y(t, q) \, \widetilde{Z}_{Y^T}(q, t) \\ & \times \prod_{s \in Y} \left(1 - Q_1 t^{-\ell_{R_1} - \frac{1}{2}} q^{-a_Y - \frac{1}{2}}\right) \left(1 - Q_2 t^{\ell_{R_2} + \frac{1}{2}} q^{a_Y + \frac{1}{2}}\right) \\ & \times \prod_{s \in R_1} \left(1 - Q_1 t^{\ell_Y + \frac{1}{2}} q^{a_{R_1} + \frac{1}{2}}\right) \prod_{s \in R_2} \left(1 - Q_2 t^{-\ell_Y - \frac{1}{2}} q^{-a_{R_2} - \frac{1}{2}}\right). \end{aligned} \tag{5.36}$$

We can observe that this function is a polynomial in Q_3 despite its appearances. It would be interesting to prove this observation. Notice that this function satisfies

$$P_{R_1,R_2}(Q_1,Q_2,Q_3,t,q) = P_{R_2,R_1}(Q_2,Q_1,Q_3,t^{-1},q^{-1}). \tag{5.37}$$

References

[1] N. Seiberg, "Five-dimensional SUSY field theories, nontrivial fixed points and string dynamics," Phys. Lett. B **388**, 753 (1996) [hep-th/9608111].

[2] M. R. Douglas, S. H. Katz and C. Vafa, "Small instantons, Del Pezzo surfaces and type I-prime theory," Nucl. Phys. B **497**, 155 (1997) [hep-th/9609071].

[3] D. R. Morrison and N. Seiberg, "Extremal transitions and five-dimensional supersymmetric field theories," Nucl. Phys. B **483**, 229 (1997) [hep-th/9609070].

[4] K. A. Intriligator, D. R. Morrison and N. Seiberg, "Five-dimensional supersymmetric gauge theories and degenerations of Calabi-Yau spaces," Nucl. Phys. B **497**, 56 (1997) [hep-th/9702198].

[5] O. Aharony and A. Hanany, "Branes, superpotentials and superconformal fixed points," Nucl. Phys. B **504**, 239 (1997) [hep-th/9704170].

[6] O. Aharony, A. Hanany and B. Kol, "Webs of (p,q) five-branes, five-dimensional field theories and grid diagrams," JHEP **9801**, 002 (1998) [hep-th/9710116].

[7] L. Bao, E. Pomoni, M. Taki and F. Yagi, "M5-Branes, Toric Diagrams and Gauge Theory Duality," JHEP **1204**, 105 (2012) [arXiv:1112.5228 [hep-th]].

[8] O. DeWolfe, A. Hanany, A. Iqbal and E. Katz, "Five-branes, seven-branes and five-dimensional (n) field theories," JHEP **9903**, 006 (1999) [hep-th/9902179].

[9] Y. Yamada and S. -K. Yang, "Affine seven-brane backgrounds and five-dimensional E(N) theories on S1," Nucl. Phys. B **566**, 642 (2000) [hep-th/9907134].

[10] T. Hauer and A. Iqbal, "Del Pezzo surfaces and affine seven-brane backgrounds," JHEP **0001**, 043 (2000) [hep-th/9910054].

[11] K. Mohri, Y. Ohtake and S. -K. Yang, "Duality between string junctions and D-branes on Del Pezzo surfaces," Nucl. Phys. B **595**, 138 (2001) [hep-th/0007243].

[12] M. R. Gaberdiel and B. Zwiebach, "Exceptional groups from open strings," Nucl. Phys. B **518**, 151 (1998) [hep-th/9709013].

[13] M. R. Gaberdiel, T. Hauer and B. Zwiebach, "Open string-string junction transitions," Nucl. Phys. B **525**, 117 (1998) [hep-th/9801205].

[14] O. DeWolfe and B. Zwiebach, "String junctions for arbitrary Lie algebra representations," Nucl. Phys. B **541**, 509 (1999) [hep-th/9804210].

[15] O. DeWolfe, T. Hauer, A. Iqbal and B. Zwiebach, "Uncovering the symmetries on [p,q] seven-branes: Beyond the Kodaira classification," Adv. Theor. Math. Phys. **3**, 1785 (1999) [hep-th/9812028].

[16] O. DeWolfe, T. Hauer, A. Iqbal and B. Zwiebach, "Uncovering infinite symmetries on [p, q] 7-branes: Kac-Moody algebras and beyond," Adv. Theor. Math. Phys. **3**, 1835 (1999) [hep-th/9812209].

[17] B. Feng, A. Hanany and Y. -H. He, "D-brane gauge theories from toric singularities and toric duality," Nucl. Phys. B **595**, 165 (2001) [hep-th/0003085].

[18] B. Feng, A. Hanany and Y. -H. He, "Phase structure of D-brane gauge theories and toric duality," JHEP **0108**, 040 (2001) [hep-th/0104259].

[19] A. Hanany and A. Iqbal, "Quiver theories from D6 branes via mirror symmetry," JHEP **0204**, 009 (2002) [hep-th/0108137].

[20] B. Feng, A. Hanany, Y. -H. He and A. M. Uranga, "Toric duality as Seiberg duality and brane diamonds," JHEP **0112**, 035 (2001) [hep-th/0109063].

[21] B. Feng, S. Franco, A. Hanany and Y. -H. He, "Symmetries of toric duality," JHEP **0212**, 076 (2002) [hep-th/0205144].

[22] B. Feng, A. Hanany, Y. H. He and A. Iqbal, "Quiver theories, soliton spectra and Picard-Lefschetz transformations," JHEP **0302**, 056 (2003) [hep-th/0206152].

[23] S. Franco and A. Hanany, "Geometric dualities in 4-D field theories and their 5-D interpretation," JHEP **0304**, 043 (2003) [hep-th/0207006].

[24] B. Feng, S. Franco, A. Hanany and Y. -H. He, "UnHiggsing the del Pezzo," JHEP **0308**, 058 (2003) [hep-th/0209228].

[25] S. Franco and A. Hanany, "Toric duality, Seiberg duality and Picard-Lefschetz transformations," Fortsch. Phys. **51**, 738 (2003) [hep-th/0212299].

[26] O. Bergman, D. Rodriguez-Gomez and G. Zafrir, "Discrete theta and the 5d superconformal index," arXiv:1310.2150 [hep-th].

[27] L. Bao, V. Mitev, E. Pomoni, M. Taki and F. Yagi, "Non-Lagrangian Theories from Brane Junctions," arXiv:1310.3841 [hep-th].

[28] H. Hayashi, H. -C. Kim and T. Nishinaka, "Topological strings and 5d T_N partition functions," arXiv:1310.3854 [hep-th].

[29] M. Taki, "Notes on Enhancement of Flavor Symmetry and 5d Superconformal Index," arXiv:1310.7509 [hep-th].

[30] O. Bergman, D. Rodriguez-Gomez and G. Zafrir, "5-Brane Webs, Symmetry Enhancement, and Duality in 5d Supersymmetric Gauge Theory," arXiv:1311.4199 [hep-th].

[31] N. A. Nekrasov, "Seiberg-Witten prepotential from instanton counting," Adv. Theor. Math. Phys. **7**, 831 (2004) [hep-th/0206161].

[32] A. Iqbal, "All genus topological string amplitudes and five-brane webs as Feynman diagrams," hep-th/0207114.

[33] A. Iqbal and A. -K. Kashani-Poor, "Instanton counting and Chern-Simons theory," Adv. Theor. Math. Phys. **7**, 457 (2004) [hep-th/0212279].

[34] M. Aganagic, A. Klemm, M. Marino and C. Vafa, "The Topological vertex," Commun. Math. Phys. **254**, 425 (2005) [hep-th/0305132].

[35] A. Iqbal and A. -K. Kashani-Poor, "The Vertex on a strip," Adv. Theor. Math. Phys. **10**, 317 (2006) [hep-th/0410174].

[36] H. Awata and H. Kanno, "Instanton counting, Macdonald functions and the moduli space of D-branes," JHEP **0505**, 039 (2005) [hep-th/0502061].

[37] A. Iqbal, C. Kozcaz and C. Vafa, "The Refined topological vertex," JHEP **0910**, 069 (2009) [hep-th/0701156].

[38] M. Taki, "Refined Topological Vertex and Instanton Counting," JHEP **0803**, 048 (2008) [arXiv:0710.1776 [hep-th]].

[39] H. Awata and H. Kanno, "Refined BPS state counting from Nekrasov's formula and Macdonald functions," Int. J. Mod. Phys. A **24**, 2253 (2009) [arXiv:0805.0191 [hep-th]].

[40] A. Iqbal and C. Kozcaz, "Refined Topological Strings and Toric Calabi-Yau Threefolds," arXiv:1210.3016 [hep-th].

[41] A. Hanany and R. -K. Seong, "Brane Tilings and Reflexive Polygons," Fortsch. Phys. **60**, 695 (2012) [arXiv:1201.2614 [hep-th]].

[42] H. -C. Kim, S. -S. Kim and K. Lee, "5-dim Superconformal Index with Enhanced En Global Symmetry," JHEP **1210**, 142 (2012) [arXiv:1206.6781 [hep-th]].

[43] A. Iqbal and C. Vafa, "BPS Degeneracies and Superconformal Index in Diverse Dimensions," arXiv:1210.3605 [hep-th].

[44] F. Benini, S. Benvenuti and Y. Tachikawa, "Webs of five-branes and N=2 superconformal field theories," JHEP **0909**, 052 (2009) [arXiv:0906.0359 [hep-th]].

[45] D. Gaiotto, "N=2 dualities," JHEP **1208**, 034 (2012) [arXiv:0904.2715 [hep-th]].

[46] M. Taki, "Flop Invariance of Refined Topological Vertex and Link Homologies," arXiv:0805.0336 [hep-th].

[47] C. Kozcaz, S. Pasquetti and N. Wyllard, "A & B model approaches to surface operators and Toda theories," JHEP **1008**, 042 (2010) [arXiv:1004.2025 [hep-th]].

[48] P. Sulkowski, "Crystal model for the closed topological vertex geometry," JHEP **0612**, 030 (2006) [hep-th/0606055].

[49] L. F. Alday, D. Gaiotto and Y. Tachikawa, "Liouville Correlation Functions from Four-dimensional Gauge Theories," Lett. Math. Phys. **91**, 167 (2010) [arXiv:0906.3219 [hep-th]].

[50] N. Wyllard, "A(N-1) conformal Toda field theory correlation functions from conformal N = 2 SU(N) quiver gauge theories," JHEP **0911**, 002 (2009) [arXiv:0907.2189 [hep-th]].

[51] D. Gaiotto, "Asymptotically free N=2 theories and irregular conformal blocks," arXiv:0908.0307 [hep-th].

[52] M. Taki, "On AGT Conjecture for Pure Super Yang-Mills and W-algebra," JHEP **1105**, 038 (2011) [arXiv:0912.4789 [hep-th]].

[53] C. A. Keller, N. Mekareeya, J. Song and Y. Tachikawa, "The ABCDEFG of Instantons and W-algebras," JHEP **1203**, 045 (2012) [arXiv:1111.5624 [hep-th]].

[54] H. Awata and Y. Yamada, "Five-dimensional AGT Conjecture and the Deformed Virasoro Algebra," JHEP **1001**, 125 (2010) [arXiv:0910.4431 [hep-th]].

[55] A. Mironov, A. Morozov, S. .Shakirov and A. Smirnov, "Proving AGT conjecture as HS duality: extension to five dimensions," Nucl. Phys. B **855**, 128 (2012) [arXiv:1105.0948 [hep-th]].

[56] F. Nieri, S. Pasquetti and F. Passerini, "3d & 5d gauge theory partition functions as q-deformed CFT correlators," arXiv:1303.2626 [hep-th].

[57] D. -E. Diaconescu and B. Florea, "The Ruled vertex and D-E degenerations," JHEP **0509**, 044 (2005) [hep-th/0507058].

[58] D. -E. Diaconescu and B. Florea, "The Ruled vertex and nontoric del Pezzo surfaces," JHEP **0612**, 028 (2006) [hep-th/0507240].

[59] K. Sakai, "Seiberg-Witten prepotential for E-string theory and random partitions," JHEP **1206**, 027 (2012) [arXiv:1203.2921 [hep-th]].

[60] K. Sakai, "Seiberg-Witten prepotential for E-string theory and global symmetries," JHEP **1209**, 077 (2012) [arXiv:1207.5739 [hep-th]].

[61] I. G. Macdonald, "Symmetric Functions and Hall Polynomials", Oxford University Press, 1998

[62] Y. Tachikawa, "Five-dimensional Chern-Simons terms and Nekrasov's instanton counting," JHEP **0402**, 050 (2004) [hep-th/0401184].